Biochimica et Biophysica Acta 1851 (2015) 1202–1217

Contents lists available at ScienceDirect

Biochimica et Biophysica Acta

journal homepage: www.elsevier.com/locate/bbalip

Unraveling fatty acid transport and activation mechanisms in *Yarrowia lipolytica*

Rémi Dulermo [a,b], Heber Gamboa-Meléndez [a,b], Rodrigo Ledesma-Amaro [a,b], France Thévenieau [c], Jean-Marc Nicaud [a,b,*]

[a] INRA, UMR1319 Micalis, F-78352 Jouy-en-Josas, France
[b] AgroParisTech, UMR Micalis, F-78352 Jouy-en-Josas, France
[c] Sofiproteol, Direction Innovation, 11 rue de Monceau, Paris F-75378, France

ARTICLE INFO

Article history:
Received 22 December 2014
Received in revised form 2 April 2015
Accepted 7 April 2015
Available online 15 April 2015

Keywords:
Peroxisome
FAT1
PXA1
PXA2
ANT1
FAA1

ABSTRACT

Fatty acid (FA) transport and activation have been extensively studied in the model yeast species *Saccharomyces cerevisiae* but have rarely been examined in oleaginous yeasts, such as *Yarrowia lipolytica*. Because the latter begins to be used in biodiesel production, understanding its FA transport and activation mechanisms is essential. We found that *Y. lipolytica* has FA transport and activation proteins similar to those of *S. cerevisiae* (Faa1p, Pxa1p, Pxa2p, Ant1p) but mechanism of FA peroxisomal transport and activation differs greatly with that of *S. cerevisiae*. While the ScPxa1p/ScPxa2p heterodimer is essential for growth on long-chain FAs, Δ*Ylpxa1* Δ*Ylpxa2* is not impaired for growth on FAs. Meanwhile, ScAnt1p and YlAnt1p are both essential for yeast growth on medium-chain FAs, suggesting they function similarly. Interestingly, we found that the Δ*Ylpxa1* Δ*Ylpxa2* Δ*Ylant1* mutant was unable to grow on short-, medium-, or long-chain FAs, suggesting that YlPxa1p, YlPxa2p, and YlAnt1p belong to two different FA degradation pathways. We also found that YlFaa1p is involved in FA storage in lipid bodies and that FA remobilization largely depended on YlFat1p, YlPxa1p and YlPxa2p. This study is the first to comprehensively examine FA intracellular transport and activation in oleaginous yeast.

1. Introduction

Peroxisomes are very important organelles that perform different metabolic functions, such as the β-oxidation of FAs and the synthesis and degradation of bioactive lipid-derived molecules. Consequently, when peroxisomes malfunction, the effects can be dramatic for cells. Indeed, the abnormal assembly of peroxisomes is responsible for Zellweger syndrome, rhizomelic chondrodysplasia punctata, and neonatal adrenoleukodystrophy in humans. In yeasts, FAs are degraded exclusively by peroxisomes, and it has been shown that the uptake of FAs into peroxisomes may occur via two routes. The first route involves the intraperoxisomal activation of free FAs into acyl-CoA esters, a process that is mediated by ScAnt1p [38,41] and ScFaa2 [21] in *Saccharomyces cerevisiae*. The second route involves two yeast half-ABC peroxisomal transporters, ScPxa1p and ScPxa2p [19], and the acyl-CoA synthetase ScFaa1 [13].

In *S. cerevisiae*, certain FAs are first activated before entering the peroxisomes. Four FA acyl-CoA synthetases, ScFaa1p to ScFaa4p, play a role in FA activation [13,20,21,26]. Indeed, ScFaa1p is essential for *S. cerevisiae* growth on media containing long-chain fatty acids (LCFAs), such as palmitate [13]. In fact, ScFaa1p and, to a lesser extent, ScFaa4p are responsible for activating exogenous FAs whereas ScFaa2p and ScFaa3p activate only endogenous FAs [20,21]. In vitro assays indicate that ScFaalp preferentially activates C12:0–C16:0 FAs such as myristic acid and pentadecanoic acid and that ScFaa2p acts on C9:0–C13:0 FAs. On the other hand, ScFaa3p is unique in that it preferentially activates C16 and C18 FAs that contain a cis double bond at C9–C10; it is also the only Faa protein that is able to activate C22:0 and C24:0 FAs. When acting on C9:0–C18:0 FAs, ScFaa3p demonstrates acyl-CoA synthetase activity that is 2- to 160-fold lower than that of ScFaalp and ScFaa2p [26]. Furthermore, [60] reported that the *S. cerevisiae* LCFA transporter ScFat1p may form complexes with ScFaa1p or ScFaa4p, which suggests that exogenous FA importation and activation are coupled in this model yeast species. Moreover, localization studies have shown that ScFaa1p is found in the plasma membrane, lipid particles, mitochondria, and the endoplasmic reticulum; ScFaa2p is found in peroxisomes and the cytosol; and ScFaa4p is found in the endoplasmic reticulum and lipid bodies [6,19,36].

Recently, [58] characterized a Faa protein, YlFaa1p (YALI0D17864p), in the oleaginous yeast, *Yarrowia lipolytica*. This protein shares about 50% identity with ScFaa1p, ScFaa4p, and ScFaa3p and only 27% identity

* Corresponding author at: Micalis Institute, INRA-AgroParisTech, UMR1319, Team BIMLip: Integrative Metabolism of Microbial Lipids, CBAI, F-78850 Thiverval-Grignon, France. Tel.: +33 130815450; fax: +33 130815457.
E-mail address: jean-marc.nicaud@grignon.inra.fr (J.-M. Nicaud).

http://dx.doi.org/10.1016/j.bbalip.2015.04.004

with ScFaa2p. The authors showed that the inactivation of *YlFAA1* (i) slightly reduced yeast growth on a rich medium; (ii) decreased acyl-CoA synthetase activity; (iii) increased the ratio of saturated to unsaturated FAs (palmitic acid/oleic acid); and (iv) increased lipid production 1.5 fold. The authors also suggested that YlFaa1p is involved in FA elongation and desaturation, a function that is not associated with *S. cerevisiae* Faa enzymes.

Once FAs have been activated, they can enter the peroxisomes. In *S. cerevisiae*, the heterodimer ScPxa1p/ScPxa2p is responsible for transporting activated LCFAs [19,49,52]. Indeed, disruption of *ScPXA1* and/or *ScPXA2* impairs yeast growth on media containing LCFAs as the sole carbon source (i.e., oleate acid and palmitate acid). Since the β-oxidation pathway is intact in these mutants, this result suggests that ScPxa1p and ScPxa2p are specifically involved in LCFA transport [19]. It was recently shown that acyl-CoA esters are hydrolyzed before being transported into the peroxisomes by ScPxa1p/ScPxa2p. Moreover, ScPxa1p/ScPxa2p transporters might be involved in some sort of functional interaction with ScFaa2p and/or ScFat1p on the inner surface of the peroxisomal membrane that results in the subsequent re-esterification of FAs with extremely long chains [44]. Because medium-chain fatty acids (MCFAs) do not need ScPxa1p/ScPxa2p transporters to enter peroxisomes, it has been suggested that they use an alternative mechanism [19].

In *S. cerevisiae*, ScAnt1p is a peroxisomal transporter whose expression is induced by oleic acid and that is essential for yeast growth in media in which MCFAs are the sole carbon source [38,41]. It mediates ATP transport into the peroxisomes; ATP is required for MCFAs to be activated and thus converted into their corresponding coenzyme A esters in the peroxisomes [29,38,41,45]. Interestingly, in *Y. lipolytica*, YlAnt1p has been described as being involved in short-chain alkane utilization (mainly of C10–C11), which suggests that activation takes place in the peroxisomes [54].

Although FA transport and activation have been extensively studied in *S. cerevisiae*, few data are available for other organisms. This is particularly true for oleaginous species such as *Y. lipolytica*, which is able to use hydrophobic substrates like oils, FAs, and alkanes as carbon sources [5]. This trait makes *Y. lipolytica* a model organism of great interest when it comes to biotechnology applications, especially biofuel production [4]. As a consequence, understanding FA transport and activation mechanisms in *Y. lipolytica* might help improve the species' production of FAs (and other related processes). In this study, we therefore aimed to explore these processes using knowledge previously gleaned from *S. cerevisiae*. We found that most of the genes involved in FA transport and activation in *S. cerevisiae* are conserved in *Y. lipolytica*; however, both processes appear to be more complex in *Y. lipolytica*. To decipher the role of these cellular mechanisms, we inactivated all the genes potentially involved in FA transport and activation in *Y. lipolytica* and analyzed their genetic interactions. We found that YlPxa1p/YlPxa2p, a homologue of ScPxa1p/ScPxa2p, may function as heterodimer; it appears to be involved in MCFA and short-chain fatty acid (SCFA) transport in addition to LCFA transport. Moreover, the deletion of *YlANT1* decreased yeast growth on SCFAs and LCFAs, and the mutant did not grow at all on C10:0 FAs, which suggests that the activation of these FAs also takes place in the peroxisomes. The absence of *YlPXA1*, *YlPXA2*, and *YlANT1* dramatically decreased yeast growth on SCFAs, MCFAs, and LCFAs. We also found that YlFaa1p is responsible for exogenous FA accumulation and that the deletion of *YlPXA1*, *YlPXA2*, and/or *YlANT1* increased FA accumulation when cells were grown in an oleate medium. Based on our results, we propose a model for FA transport and activation in different cellular compartments in *Y. lipolytica*.

2. Material and methods

2.1. Yeast strains and culture conditions

The *Y. lipolytica* strains used in this study were derived from the wild-type *Y. lipolytica* strain W29 (ATCC20460) (Table 1). The auxotrophic strain used here, Po1d (Leu− Ura−), was previously described by [2]. All the strains used in this study are listed in Table 1. The media and growth conditions for *Escherichia coli* in this study are the same as those of [47], and the conditions for *Y. lipolytica* are the same as those of [2]. Rich medium (YPD) and minimal glucose medium (YNB) were prepared as described in [33]. The YNB medium contained a 0.17% (wt/vol) yeast nitrogen base (without amino acids or ammonium sulfate, YNBww; Difco, Paris, France), 0.5% (wt/vol) NH_4Cl, and a 50 mM phosphate buffer (pH 6.8). As necessary, the YNB medium was supplemented with uracil (0.1 g/L) and/or leucine (0.1 g/L). The $YNBD_{0.5}O_3$ medium contained 0.1% (wt/vol) yeast extract (Bacto-BD), 0.5% glucose, and 3% oleic acid. Solid media were created by adding 1.6% agar. The $YNBC_0$ medium was prepared in the same way as the YNB medium

Table 1
Strains and plasmids.

Strain or plasmid	Genotype or other relevant characteristics	Source or reference
E. coli		
DH5α	*Φ80dlacZΔm15*, *recA1*, *endA1*, *gyrA96*, *thi-1*, *hsdR17* (r_k-, m_k+), *supE44*, *relA1*, *deoR*, *Δ(lacZYA-argF)U169*	Promega
Y. lipolytica		
W29	*MATA*, *wild-type*	[2]
Po1d	*MATA ura3*–302 *leu2*–270 *xpr2*–322	[2]
JMY330	Po1d Ura+	[18]
JMY2900	Po1d Ura + Leu+	[12]
JMY2954	Po1d Δ*Ylpxa1*::*URA3ex*	This study
JMY2959	Po1d Δ*Ylpxa2*::*URA3ex*	This study
JMY2964	Po1d Δ*Ylfaa1*::*URA3ex*	This study
JMY2969	Po1d Δ*Ylant1*::*URA3ex*	This study
JMY3159	Y2954 + Δ*Ylpxa2*::*LEU2ex*	This study
JMY3230	Y2954 + *LEU2ex*	This study
JMY3233	Y2959 + *LEU2ex*	This study
JMY3234	Y2964 + *LEU2ex*	This study
JMY3237	Y2969 + *LEU2ex*	This study
JMY3240	JMY3148 + *LEU2*ex (Ura^+ Leu^+)	[12]
JMY3464	Y2964 + Δ*Ylant1*::*LEU2ex*	This study
JMY3670	Y2969 p*TEF-YlANT1-LEU2ex*	This study
JMY3701	Y3159 Ura− Leu−	This study
JMY3737	Y3701 + Δ*Ylant1*::*LEU2ex*	This study
JMY3795	Y3737 + *URA3ex*	This study
JMY3797	Y2954 + Δ*Ylant1*::*LEU2ex*	This study
JMY3811	Y2959 + Δ*Ylant1*::*LEU2ex*	This study
JMY4138	Y3737 + Δ*Ylfat1*::*URA3ex*	This study
JMY4150	Y3701 + Δ*Ylfat1*::*URA3ex*	This study
JMY4160	Y4150 + *LEU2ex*	This study
JMY4194	Y2954 + p*TEF-YlPXA1-YFP-LEU2ex*	This study
JMY4251	Y4194 Ura− Leu−	This study
JMY4253	Y2959 + p*TEF-YlPXA2-YFP-LEU2ex*	This study
JMY4255	Y2964 + p*TEF-YlFAA1-YFP-LEU2ex*	This study
JMY4258	Y4251 + p*TEF-RedStar2-SKL-LEU2ex*	This study
JMY4297	Y4253 Ura + Leu−	This study
JMY4327	Y4297 + p*TEF-RedStar2SKL-LEU2ex*	This study
pCR4Blunt-TOPO	Cloning vector	Invitrogen
JMP547	pUB4-CRE	[15]
JMP803	JMP62-p*TEF-URA3*ex	[35,37]
JMP802	JMP62-p*TEF-LEU2*ex	[18]
JMP1392	JMP62-p*TEF-RedStar2SKL-LEU2ex*	[23]
JMP1394	JMP62-p*TEF-RedStar2-LEU2ex*	T. Rossignol, unpublished data
JMP1762	pCR4Blunt-TOPO-*Ylfat1*::*URA3ex*	[12]
JMP1673	Topo *YlPXA2*UpDn-*URA3ex*	This study
JMP1675	Topo *YlFAA1*UpDn-*URA3ex*	This study
JMP1676	Topo*YlANT1*UpDn-*URA3ex*	This study
JMP1697	Topo *YlPXA1*UpDn-*URA3ex*	This study
JMP1765	Topo *YlPXA2*UpDn-*LEU2ex*	This study
JMP1842	Topo *YlANT1*UpDn *LEU2ex*	This study
JMP1929	Topo *YlFAA1*	This study
JMP1934	Topo *YlANT1*	This study
JMP2025	JMP62 p*TEF-YlANT1-LEU2ex*	This study
JMP2384	JMP62 + p*TEF-YlPXA1-YFP-LEU2ex*	This study
JMP2387	JMP62 + p*TEF- YlPXA2-YFP-LEU2ex*	This study
JMP2390	JMP62 + p*TEF- YlFAA1-YFP-LEU2ex*	This study

except that no carbon source was added [11]. When fatty acids were included in liquid or solid media, a 50:50 emulsion of fatty acids/10% pluronic acid was prepared and then heated at 80 °C for 10 min before being added to the media. The following fatty acids were used in our study: C6:0 (Sigma Aldrich, 99%), C10:0 (Sigma Aldrich, 99%), and C18:1 (Sigma Aldrich, 70%). $YNBD_{0.5}O_3$ and $YNBC_0$ media were used for the lipid accumulation and lipid remobilization experiments, respectively.

2.2. Construction of plasmids and strains

Primarily, the deletion cassettes were generated using PCR amplification according to the procedure used by [15]. First, the upstream (Up or P) and downstream (Dn or T) regions were amplified from *Y. lipolytica* W29 genomic DNA; they were used as templates and the gene-specific Up and Dn oligonucleotides served as primer pairs (Table 2). The primers UpISceI or P2ISceI and DnISceI or T1ISceI contained extensions used to introduce the I-SceI restriction site that allowed an UpDn fragment to be constructed employing PCR fusion (see above).

To disrupt *YlANT1* (*YALI0E03058*), the primer pairs E03058UpNotI/E03058UpISceI and E03058DnNotI/E03058DnISceIIceuI were used (Table 2). The Up and Dn regions were purified and then used for the PCR fusion. The resulting UpDn fragment was ligated into pCR4Blunt-TOPO, yielding the strain JMP1644. The *URA3* and *LEU2* markers (from JMP802 and JMP803) were then introduced at the I-SceI site, yielding JMP1677 and JME1842, which contained, respectively, the *YlANT1::URA3* and *YlANT1::LEU2* cassettes. The deletion cassettes were released from the plasmids by *Not*I digestion.

To disrupt *YlFAA1* (*YALI0D17864*), the primer pairs D17864UpNotI/D17864UpISceI and D17864DnNotI/D17864DnISceIIceuI were used

Table 2
List of primers.

Genes	Primers	Sequences	Utilization
YlPXA1	A06655Up2NotI	GAATGCGGCCGCCCTTTCATATGGAATGCTCACCACACC	Upstream fragment of *YlPXA1*
YlPXA2	A06655Up2IsceI	CGATTACCCTGTTATCCCTACCGGGGTCTTGAGAGCTGTGGCTAC	
	A06655Dn2NotI	GAATGCGGCCGCCAATTGCAGCACCCAGGATTCTCG	Downstream fragment of *YlPXA1*
	A06655Dn2IsceIIceuI	GGTAGGGATAACAGGGTAATCGTAACTATAACGGTCCTAAGGTAGCGATATC GATTCCTGTTTGTATGTATGTTCGC	
	Ver1A06655	CTCAGCCTCTGATAGCGTGG	Verification of disruption
	Ver2A06655	AGCAAGTTACGCCTTACACC	
	A06655BamHI2	ATCGGATCCCACAATGGCAAACGTCTCTACACTACGACCGCTGCTCATCGAGG	Construction of the *YlPXA1-YFP* fusion in JMP1427
	A06655Rbis	CCACACTCAGACGAGCCTCCTTGGAACCCACAATCTCAAGATCCCAGTCC	
	A06655Fbis	GGACTGGGATCTTGAGATTGTGGGTTCCAAGGAGGCTCGTCTGAGTGTGG	
	A06655AvrIIF	CATCCTAGGTTCTTCTCGGACTTCTTGGGATTGCTAGTCTTGG	
	A06655F	GGAAGGATGTCTTTTCTGG	*YlPXA1* expression by RT-PCR
	A06655R	AAGGTCGATGAGATATGGTG	
	D04246UpNotI	GAATGCGGCCGCATGGCATACATCACTTGTCC	Upstream fragment of *YlPXA2*
	D04246UpIsceI	CGATTACCCTGTTATCCCTACCGTTTTGAGACGGTCCATCTG	
	D04246DnNotI	GAATGCGGCCGCGCCACCAACTTCTCTTACTG	Downstream fragment of *YlPXA2*
	D04246DnIsceIIceuI	GGTAGGGATAACAGGGTAATCGTAACTATAACGGTCCTAAGGTAGCGAGGGT GCGAAGATTACGACG	
	Ver1D04246	CGTCATTGTTGTTCTCCTGG	Verification of disruption
	Ver2D04246	TCGGCTACTACCCTGGCGTC	
	D04246BamHI2	ATCGGATCCCACAATGGACCGTCTCAAAACGTCGGCTGTGGGC	Construction of the *YlPXA2-YFP* fusion in JMP1427
	D04246AvrIIF2	CATCCTAGGTGAGCAACAGACGCCTTGAGCATTGCTAGACGTTCTTCC	
	D04246F	TTCTACCACAAGCCGAAG	*YlPXA2* expression by RT-PCR
	D04246R	TCGCCAAAGAGATAACCA	
YlFAA1	D17864UpNotI	GAATGCGGCCGCTGCTCATCTCACTCGTACGC	Upstream fragment of *YlFAA1*
	D17864UpIsceI	CGATTACCCTGTTATCCCTACCCCATTCTTTGTTAGTTGTTGG	
	D17864DnNotI	GAATGCGGCCGCATCTTCCATCGATACCAACC	Downstream fragment of *YlFAA1*
	D17864DnIsceIIceuI	GGTAGGGATAACAGGGTAATCGTAACTATAACGGTCCTAAGGTAGCGACGA GCAGTCTTAGAGTGTT	
	Ver1-1D17864	GCCAATGGTTGCGCATTTCCCGG	Verification of disruption
	Ver2-2D17864	GTTCCAGCAACAGACTGACAGC	
	D17864BamHI2	ATCGGATCCCACAATGGTCGGATACACAATTTCCTCAAAGCCCG	Construction of the *YlFAA1-YFP* fusion in JMP1427
	D17864AvrII2	CATCCTAGGGACTGCTCGTAGCACTCATCAATTTCCTTCTTG	
	D17864F	GTGATATTGCCGAGTGGA	*YlFAA1* expression by RT-PCR
	D17864R	CTCGTTAGGAATGACCAGAG	
YlANT1	E03058UpNotI	GAATGCGGCCGCACGTGCGATCTGTGGATTTC	Upstream fragment of *YlANT1*
	E03058UpIsceI	CGATTACCCTGTTATCCCTACCTGAGTGAGATGGGTGAGTTG	
	E03058DnNotI	GAATGCGGCCGCCCATAGTGGCCAGTCATC	Downstream fragment of *YlANT1*
	E03058DnIsceIIceuI	GGTAGGGATAACAGGGTAATCGTAACTATAACGGTCCTAAGGTAGCGACAAGGGA TAAGAATAGACAAGAC	
	Ver1E03058	CCGTTCTGCTCCAGGGTAAC	Verification of disruption
	Ver2E03058	ACACTCTTATGCCGGACCGC	
	E03058FYFP2	CGGCATGGACGAGCTGTACAAGATGGCAGCTATTTCCAAAGACTATGTTCTGTCG	Construction of the *YlANT1-YFP* fusion protein
	E03058AvrII3	CATCCTAGGTTATCCCTTGATCAAGGTGGGGGCCTTCATG	
	YFPBamHI2	ATCGGATCCCACAATGAAGCTTCCCCGCGGCCTAGG	
	YFPFE03058	CATAGTCTTTGGAAATAGCTGCCATCTTGTACAGCTCGTCCATGCCG	
	E03058F	TCCCTCTTGTCTTCTAGGTGT	*YlANT1* expression by RT-PCR
	E03058R	AGTCTGCTGTCGTGTGGT	
ACTIN	ACT-A1	TCCAGGCCGTCCTCTCCC	*Actin* expression by RT-PCR
	ACT-A2	GGCCAGCCATATCGAGTCGCA	
ALG9	ALG9-A1	AGTATCCCTCTGCACATGA	*ALG9* expression by RT-PCR
	ALG9-A2	TTGGCAGGAATATCGATGTC	
	pTEF-start	GGGTATAAAAGACCACCGTCC	Verification of the insertion of the overexpression cassette into the *Y. lipolytica* genome
	61 stop	GTAGATAGTTGAGGTAGAAGTTG	

(Table 2). The Up and Dn regions were purified and then used for the PCR fusion. The resulting UpDn fragment was ligated into pCR4Blunt-TOPO, yielding JMP1643. The *URA3* marker (from JMP803) was then introduced at the I-SceI site, yielding JMP1675, which contained the *YlFAA1::URA3* cassette. The deletion cassettes were released from the plasmids by *Not*I digestion.

To disrupt *YlPXA1* (*YALI0A06655*), the primer pairs A06655Up2NotI/A06655UpIsceI and A06655Dn2NotI/A06655Dn2IsceIIceuI were used (Table 2). The Up and Dn regions were purified and then used for the PCR fusion. The resulting UpDn fragment was ligated into pCR4Blunt-TOPO, yielding JMP1633. The *URA3* marker (from JMP803) was then introduced at the I-SceI site, yielding JMP1697, which contained the *YlPXA1::URA3* cassette. The deletion cassettes were released from the plasmids by *Not*I digestion.

To disrupt *YlPXA2*, the primer pairs D04246UpNotI/D04246UpIsceI and D04246DnNotI/D04246DnIsceIIceuI were used (Table 2). The Up and Dn regions were purified and then used for the PCR fusion. The resulting UpDn fragment was ligated into pCR4Blunt-TOPO, yielding JMP1637. The *URA3* and *LEU2* markers (from JMP802 and JMP803) were then introduced at the I-SceI site, yielding JMP1673 and JME1765, which contained, respectively, the *YlPXA2::URA3* and *YlPXA2::LEU2* cassettes. The deletion cassettes were released from the plasmids by *Not*I digestion.

Cassettes for the complementation of Δ*Ylant1*, Δ*Ylpxa1*, Δ*Ylpxa2*, and Δ*Ylfaa1* were constructed using the primer pairs E03058Start/E03058End, A06655BamHI2/A06655AvrIIF, D04246BamHI2/D04246AvrIIF2, and D17864BamHI2/D17864AvrII2, respectively. The *YlPXA1* ORF was acquired by the fusion of two PCR fragments obtained with primer pairs A06655BamHI2/A06655Rbis and A06655Fbis/A06655AvrIIF. The *YlANT1* ORF was cloned into pCR4Blunt-TOPO (JME1934) and then digested by *Avr*II and *Bam*HI. It was then cloned into a form of JMP1394 previously digested by *Bam*HI and *Avr*II to yield JME2025. The PCR fragments of the other genes were digested by *Bam*HI and *Avr*II and cloned into JMP1427 to yield JMP2384, JMP2387, and JMP2390, respectively.

Transformation involving the disruption or overexpression cassettes was performed using the lithium acetate method [30]. Transformants were selected on YNBcasa, YNBura, or YNB media, depending on the genotype of interest. Then genomic DNA from the yeast transformants was prepared as described by [40]. The corresponding ver1 and ver2 primers (Table 2) were used to verify gene disruption, and the pTEF start and 61 stop primers were used to verify integration of the overexpression cassette. To delete more than two genes, markers were excised using JMP547 as already described in [15].

Restriction enzymes were obtained from OZYME (Saint-Quentin-en-Yvelines, France). The PCR amplifications were performed using an Eppendorf 2720 thermal cycler and employing GoTaq DNA polymerases (Promega, Madison, WI) for PCR verification and PyroBest DNA polymerases (Takara, Saint-Germain-en-Laye, France) for cloning. The PCR fragments were purified using a QIAgen Purification Kit (Qiagen, Hilden, Germany), and the DNA fragments were recovered from the agarose gels using a QIAquick Gel Extraction Kit (Qiagen, Hilden, Germany). Amount of DNA were measure by a MySpec (VWR, Fontenay-sous-Bois, France). All the procedures were carried out in accordance with the manufacturers' instructions. The Clone Manager software package was used for the gene sequence analysis (Sci-Ed Software, Morrisville, NC).

2.3. Gas chromatography

Lipids were extracted from 10–20 mg aliquots of cells and converted into their equivalent methyl esters using the procedure described in [7]. The products were then used in the gas chromatography analysis. This analysis was performed using a Varian 3900 gas chromatograph equipped with a flame ionization detector and a Varian FactorFour vf-23 ms column, where the bleed specification at 260 °C was 3 pA (30 m, 0.25 mm, 0.25 μm). FA were identified by comparison with commercial fatty acid methyl ester standards (FAME32, Supelco) and quantified by the internal standard method with the addition of 50 μg of commercial C17:0 (Sigma, Saint-Quentin Fallavier, France).

2.4. FFA and TAG amounts determination

Lipids from aliquots of 10 mg of cells were extracted by the procedure of Folch et al. [61] for HPLC analysis. Lipid species were analyzed using a gradient reversed phase HPLC (Ultimate 3000, Dionex-Thermo Fisher Scientific, UK) using an Acclaim™ 120 C8 3 μm 120 Å coupled to a Corona Veo detector. The column was eluted with a binary gradient solution (Table S1) at 40 °C and a constant flow rate of 0.8 ml min^{-1}. Identification and quantification were achieved via comparisons to standards.

2.5. Analysis of the expression of YlPXA1, YlPXA2, YlANT1, and YlFAA1

To determine if oleate induced the expression of *YlPXA1*, *YlPXA2*, *YlANT1*, and *YlFAA1*, precultures of the reference strain (JMY2900) were set up in liquid YNB, supplemented with 1% glucose and 0.5% yeast extract, and grown for 15 h at 28 °C. Cells were washed with distilled water and transferred to a fresh liquid YNB medium supplemented with 1% glucose, 3% oleate, or both 1% glucose and 3% oleate. Cultures were grown in baffled Erlenmeyer flasks kept at 28 °C and 160 rpm. Cells were harvested at 2 and 6 h post inoculation, frozen in liquid nitrogen, and stored at −80 °C. RNA was extracted from the cells using the RNeasy Mini Kit (Qiagen, Hilden, Germany), and 2 μg were treated with DNAse (Ambion, Life Technologies, Saint Aubin, France). cDNA was synthesized using the SuperScript III First-Strand RT-PCR Kit (Invitrogen, Saint Aubin, France). PCR was then performed using the GoTaq DNA Polymerase Kit (Promega, Madison, W) employing specific primers designed by the Primer3 program (see Table 2).

2.6. Microscopic analysis

Images were acquired using a Zeiss Axio Imager M2 microscope (Zeiss, Le Pecq, France) equipped with a 100× objective lens and Zeiss filters 45 and 46 for fluorescent microscopy. Axiovision 4.8 software (Zeiss, Le Pecq, France) was used for image acquisition. Lipid bodies were visualized after adding BodiPy® Lipid Probe (2.5 mg/ml in ethanol; Invitrogen, Saint Aubin, France) to the cell suspension (A_{600} of 5) and after incubating the cells at room temperature for 10 min. The LIVE/DEAD BacLight Bacterial Viability Kit (Life Technologies) was used as per the manufacturer's instructions to count living and dead cells under the microscope.

2.7. In silico flux balance analysis

Flux balance analysis calculations were performed using MATLAB (Mathworks, Natick, MA) and the Raven toolbox [1]. To determine if the model can predict growth the reaction 'BiomassEx' was set as the objective function and the system of linear equations was solved. Fatty acids uptake (C18:1, C10 and C6) were constrained to 1 mmol/gh. For analyzing the capacity to produce lipid bodies, the reaction 'LipidBodyExcretion' was the objective function. In order to simulate the different knock outs strains the flux carried by the reactions associated to the studied genes (ant1, faa1, pxa1, pxa2 and fat1) were set to zero. The absences of fluxes in the reactions to produce biomass or lipid bodies were associated to the incapability of that genotype either to grow or to produce lipid bodies. The Biomet toolbox 2.0 (http://biomet-toolbox.org/) on line tool was used to check the flux balance analysis [22].


YlPxa1p ----MANVSTLRPLLIEALQDPVKLRA-------FISTYLASLRQMSP--------RRLR 41
ScPxa1p MSTTLAAPAKLKSLLLNLHTHCIGLHVNDVTPKVYFKLLIRHLLQISRSNAAHPKLRRRA 60
TM1
YlPxa1p VIAVVAFLLVGSCTG----------IAGQALLDNLNTKKSKKKVPLHRMDSAVKLSDGSK 91
ScPxa1p QILLVSLFLSGVTLFSGVTYSTFKIILKCYKFYKFPWKRRNRRPLIRRTRSQMQLDSGAR 120
TM1
YlPxa1p QIVVPYKEGQTTVTIKPTKQVTFEAHR---RLFLRPDDS---------------EGGEAK 133
ScPxa1p IMYIPEVELVDRQSPDDNKFMNATDKKKRKRIFIPPKDNDVYEHDKFLFKNVELERAKNS 180
TM2
TM2
YlPxa1p SGINGRFLRQFSALWVIMVPRLQSRESLILLVHALFLFLRTWISLLVAKLDGQIVRDMIA 193
ScPxa1p QLFYSKFLNQMNVLSKILIPTVFDKNFLLLTAQIFFLVMRTWLSLFVAKLDGQIVKNIIA 240
TM3
TM3
YlPxa1p GDGRKFLRGLGYWFAIAVPASYTNAVIKYLQAKLSLAFRTRLTRYVHDLYLDADLAYYKI 253
ScPxa1p GRGRSFLWDLGCWFLIAVPASYTNSAIKLLQRKLSLNFRVNLTRYIHDMYLDKRLTFYKL 300
TM3
YlPxa1p ADIDGGN--VGTSADQFITTDLARFCDKAAALYSNLGKPFVDFLIFTFQLSKNLGPMALI 311
ScPxa1p IFDAKASNSVIKNIDNSITNDVAKFCDATCSVFANIAKPVIDLIFFSVYLRDNLGTVGVA 360
TM4
TM4
YlPxa1p GIFANYGLTAYLLRRLAPSFGKLAAIQAKLEGEYRAAHSKLITNAEEIAFYDGTSLERTI 371
ScPxa1p GIFVNYFITGFILRKYTPPLGKLAGERSASDGDYYNYHLNMINNSEEIAFYQGTAVERTK 420
TM4
TM5
TM5
YlPxa1p LEKAYIRLARHIRGIYRIKIFYNMFEDIILKYTWSAIGYMFASLPVFLPAWTSIKEKTKE 431
ScPxa1p VKELYDVLMEKMLLVDKVKFGYNMLEDYVLKYTWSGLGYVFASIPIVMSTLATGIN---- 476
TM5
YlPxa1p TTASAVTASMDFSEQDHMRDFITNKRLMLSLADAGGRMMYSIKDLAELSGYTSRVYMLLS 491
ScPxa1p ----------SEEKNMKEFIVNKRLMLSLADAGSRLMHSIKDISQLTGYTNRIFTLLS 524
YlPxa1p VLHRVHARAYTSRILKTPIKEAASKEAKEEGIVIGEKPDPDSSSELSEEEQFTLNSISGT 551
ScPxa1p VLHRVHSLNFNYGAVPS--------------ILSIRTEDASRNSNLLPTTDNSQDAIRGT 570
YlPxa1p IQPRYPGVRFEGVPIVAPSAVGSGELLVR----------------------------D 581
ScPxa1p IQRNFNGIRLENIDVIIPSVRASEGIKLINKLTFQIPLHIDPITSKSNSIQDLSKANDIK 630
YlPxa1p LNVLIKPGEHILISGPNGCGKSAVARVIGGLWPVYR--GLLSRPDISEIGFLPQRAYLSI 639
ScPxa1p LPFLQGSGSSLLILGPNGCGKSSIQRIIAEIWPVYNKNGLLSIPSENNIFFIPQKPYFSR 690
YlPxa1p G-SLRDQIIYPDSHADMISKNVTDADLQTILDRVHLGYLPSREGGWN---TRKEWKDVFS 695
ScPxa1p GGTLRDQIIYPMSSDEFFDRGFRDKELVQILVEVKLDYLLKRGVGLTYLDAIADWKDLLS 750
YlPxa1p GGEKQRVMFARILYHRPKFAVIDEGTAAVSSDVEGSLYENCKKDGITLITISHRPSLMKY 755
ScPxa1p GGEKQRVNFARIMFHKPLYVVLDEATNAISVDMEDYLFNLLKRYRFNFISISQRPTLIKY 810
YlPxa1p HKAQLKLGLGNDGKDWDLEIVGSKEARLSVEKEIQSLEEKLSKVDEWKKRKTEVEAILRG 815
ScPxa1p HEMLLEIGENRDGK-WQLQAVGTDEAITSIDNEIEELERKLERVKGWEDERTKLREKLEI 869
YlPxa1p EVKHEQKPGFQEIVTENVQNTGDDTGVLLKTDTIVGVGKESEEEDVKEMKQQLGSVVKAE 875
ScPxa1p I---------- 870
YlPxa1p GDAAVKEQAAKELNEATEKLEAAKEKTDKGDVKVEGGADKPAAAKTSNPKKSEKK 930
ScPxa1p ----------

3. Results and discussion

3.1. Transport and activation mechanisms found in S. cerevisiae are conserved in Y. lipolytica

In order to know if *Y. lipolytica* contains the same set of FA transport and activation genes as *S. cerevisiae*, we searched for gene homologues. Although *S. cerevisiae* possesses four Faap proteins as well as one Fat1p and one Ant1p protein, *Y. lipolytica* has only one Faap protein, one Fat1p protein [12], and three potential Ant1p proteins. Indeed, YlAnt1p (YALI0E3058p) has two homologues in *Y. lipolytica*: YALI0A20944p (34% shared identity) and YALI0C06127p (32% shared identity). According to annotation data, YALI0A20944p is related to the peroxisomal membrane protein PMP47B found in *Neurospora crassa* (Génolevure), which is involved in peroxisome metabolism [46], and YALI0C06127p is related to Flx1p in *S. cerevisiae* (Génolevure), a carrier protein involved in maintaining a proper balance of flavin nucleotides in mitochondria [56].

To expand our search, we looked for ScPxa1p and ScPxa2p homologues in the *Y. lipolytica* genome. Blast analysis revealed that *Y. lipolytica* possesses two proteins, YALI0A06655p (which has been named YlPxa1p) and YALI0D04246p (which has been named YlPxa2p), that are homologous to ScPxa1p (41% shared identity) and ScPxa2p (35% shared identity), respectively. The alignments of YlPxa1p with ScPxa1p and Ylpxa2p with ScPxa2p are shown in Figs. 1 and 2. As for ScPxa1p, five transmembrane domains (TMs) were predicted by TMHMM for YlPxa1p (Fig. 1); only four were predicted for YlPxa2p based on the five identified for ScPxa2p (Fig. 2). The residues most conserved between YlPxa1p and ScPxa1p are found in the following areas: loop 1, the EAA-like motif (found in some transporters), the Walker A and B motifs (generally found in transporters), and the C sequence (sequence located immediately after the N-terminal of the Walker B motif). It has been shown that highly conserved residues like E294 (E357 for YlPxa1p and E406 for ScPxa1p; Fig. 1) and G301 (G364 for YlPxa1p and G413 for ScPxa1p; Fig. 1) of the EAA motif and R108 (R173 for YlPxa1p and R220 for ScPxa1p; Fig. 1) of loop 1 are essential for ScPxa1p activity [49]. These amino acid sequences are conserved not only in *Y. lipolytica* and *S. cerevisiae*, but also in the human homologue of ScPxa1p: ABCD1 (also called ALDP). Indeed, mutations of these residues are associated with adrenoleukodystrophy (Fig. 1; [49]); other mutations in the human form of Pxa1p, such as the transformation of a Gly_{512} residue into a Ser (e.g., G601 in YlPxa1p) or a Ser_{606} residue into a Leu (e.g., S695 in YlPxa1p), decrease ATPase activity and ATP binding affinity, respectively (www.uniprot.org/uniprot/P33897). Surprisingly, analyses of YlPxa2p by Mitoprot predicted a putative mitochondrial localization with the following mitochondria-targetting sequence MDRLKTSAVGQKVVSYVSARSPVWGATYLRH (Fig. 2).

3.2. Expression of YlANT1, YlPXA1, YlPXA2, and YlFAA1 is induced by oleate

We had already found that the expression of *YlFAT1* and *YlPEX11*, two genes involved in lipid metabolism, is induced by oleic acid ([12]; unpublished data). In order to determine if the expression of *YlANT1*, *YlPXA1*, *YlPXA2*, and *YlFAA1* is also regulated by oleic acid, we used the following procedure. *Y. lipolytica* cells were grown in YNB medium containing 1% glucose; they were then transferred to YNB medium supplemented with 1% glucose or 3% oleate, or both 1% glucose and 3% oleate. RT-PCR analysis performed after 2 and 6 h of growth indicated that (i) *YlANT1*, *YlPXA1*, *YlPXA2*, and *YlFAA1* were expressed under all the conditions tested and (ii) these genes were upregulated in media containing oleate (Fig. 3). These results are similar to those obtained for *S. cerevisiae* cultivated in oleic acid [45,51,57]. Moreover, our results show that the presence of glucose does not repress the upregulation of these genes by oleate and strongly suggest that YlAnt1p, YlPxa1p, YlPxa2p, and YlFaa1p play a role in oleate utilization.

3.3. Localization of YlPxa1p, YlPxa2p, and YlFaa1p

In *S. cerevisiae*, ScPxa1p, ScPxa2p, and ScAnt1p are found in peroxisomes [19,49,52], while ScFaa1p is found in the plasma membrane, lipid particles, mitochondria, and the endoplasmic reticulum [6,19,36]. To determine whether YlPxa1p, YlPxa2p, YlAnt1p, and YlFaa1p occur in those same locations in *Y. lipolytica*, four YFP fusion proteins were added to the C-terminals of YlPxa1p, YlPxa2p, and YlFaa1p (YlPxa1-YFPp, YlPxa2-YFPp, and YlFaa1-YFPp) and the N-terminal of YlAnt1p (YFP-YlAnt1p). We could not characterize the localization patterns of YlAnt1p because we could not obtain a functional fusion protein (data not shown). All the other constructs were functional and complemented the original phenotype (see above as well as Figs. 8 and 9). YlPxa1-YFPp and YlPxa2-YFPp are localized in peroxisome (Fig. 4). Confirmation of peroxisomal localisation was obtained by introducing a *RedStar2SKL*, which targets peroxisome, into these strains since co-localisation of both tagged-proteins was observed (Fig. 4). Our results also show that, contrary to Mitoprot's prediction, YlPxa2p is not found in mitochondria. YlFaa1-YFPp occurred around lipid bodies, cytoplasm and in the vacuole (Fig. 4). It is most likely that partial YlFaa1-YFPp accumulation in the vacuole is due to its overexpression. These results suggest that FA activation in the cytoplasm and FA transport into the peroxisomes could be similar in *Y. lipolytica* and *S. cerevisiae*.

3.4. YlANT1, but not YlPXA1, YlPXA2, or YlFAA1, is essential for growth on FAs

To analyze the role of *YlANT1*, *YlPXA1*, *YlPXA2*, and *YlFAA1* in FA utilization, single mutants were constructed (JMY3237, JMY3230, JMY3233, and JMY3234, respectively). All the mutants grew as well as the reference strain (JMY2900) in the presence of glucose (data not shown). The growth capacity of these strains was tested using plates containing different FAs—C6:0, C10:0, and C18:1—and dicarboxylic acid (DC18:1), as the sole carbon source. *Y. lipolytica* is able to degrade and to produce dicarboxylic acids [17,50,53]. It was also show previously that the acyl-CoA oxydases Aox1p and Aox2p were involved in dicarboxylic acids degradation while Aox2p to Aox5p were involved in fatty acids degradation with a chain-length specificity [53,55]. Therefore the dicarboxylic acid CD18:1 was included in this study. Surprisingly, Δ*Ylpxa1* and Δ*Ylpxa2* grew as well as the parental strain (Fig. 5), suggesting that at least one other protein is present and compensates for the absence of YlPxa1p or YlPxa2p. This could include transporters of activated or unactivated FAs; however, in this later case, this finding means that FA activation takes place in the peroxisomes. Moreover, since ScPxa1p and ScPxa2p form a heterodimer in *S. cerevisiae* [19,52], another hypothesis that could explain our results is that, in *Y. lipolytica*, YlPxa1p or YlPxa2p form a functional homodimer and that the absence of one protein is compensated for by the presence of the other. This last hypothesis is possible since the Pxa1 and Pxa2 human homologues—ABCD1, ABCD2, and ABCD3—function as homodimers [31,42,43,62].

Interestingly, Δ*Ylant1* failed to grow at all on C10:0; its growth demonstrated a strong decrease on C6:0 and DC18:1 and a slight decreases on C18:1 (Fig. 5). A slight decrease in growth associated with C18:1 was also observed when the mutant was grown in a liquid medium (Fig. S1A). To confirm that the phenotype of the Δ*Ylant1* mutant was really due to the gene deletion, complementation was performed by

Fig. 1. Alignment of YlPxa1p with ScPxa1p. The alignment was performed using ClustalW. The yellow frame corresponds to loop 1; the blue frame to the EAA-like motif; the green frame to the Walker A motif; the black frame to the C sequence; and the orange frame to the Walker B motif (from [49]). The residues that are underlined and in slightly bigger font are the mutated residues found in people afflicted with peroxisome Pxa1 disease (www.uniprot.org/uniprot/P33897). The black lines and the green lines indicate the positions of the potential transmembrane domains (TMs) in YlPxa1p and ScPxa1p, respectively; these were identified using TMHMM v.2 (www.cbs.dtu.dk/services/TMHMM/). Their probabilities range from 0.8 to 1 for YlPxa1p and from 0.7 to 1 for ScPxa1p.

Fig. 2. Alignment of YlPxa2p with ScPxa2p. The alignment was performed using ClustalW. The arrow indicates the potential cleavage site for the mitochondria-targeting sequence given by Mitoprot (http://ihg.gsf.de/ihg/mitoprot.html). The black lines and the green lines indicate the positions of the potential transmembrane domains (TMs) in YlPxa2p and ScPxa2p, respectively; these were identified using TMHMM v.2 (www.cbs.dtu.dk/services/TMHMM/). Their probabilities range from 0.9 to close to 1 for YlPxa2p and from 0.3 to 0.8 for ScPxa2p.

constitutively expressing *YlANT1* under the p*TEF* promoter. As expected, the mutant strain was able to grow as the parental strain on all the FAs tested (data not shown). These results show that MCFA (C10:0 here) are only activated in the peroxisomes, as previously demonstrated in *S. cerevisiae*, where ScAnt1p was necessary for yeast growth on C8 and C12 [38,41]. These results concur with those obtained by [54]: medium-chain alkanes (C10 and C11) require the presence of YlAnt1p to be consumed.

The deletion of *YlFAA1* had little to no effect on yeast growth on FAs excepted on C18:1 (Fig. 5 and Fig. S1A). Although we cannot exclude the

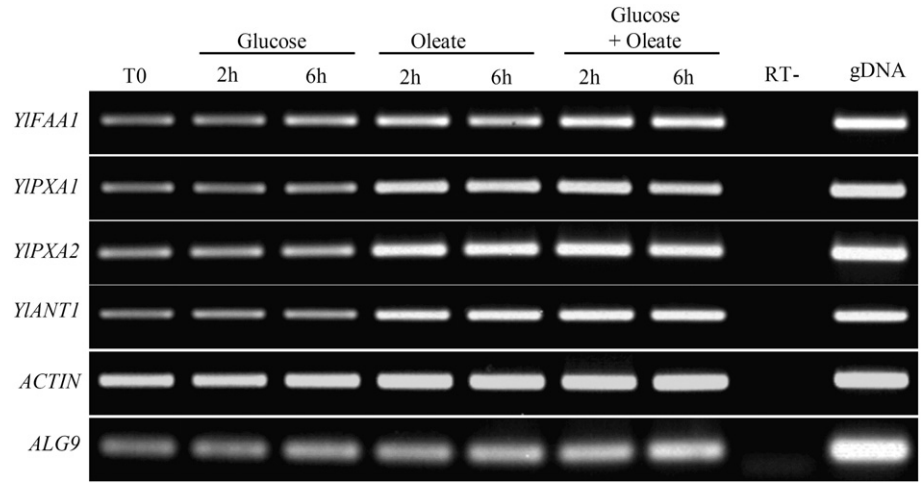

Fig. 3. Expression profiles for YlFAA1, YlPXA1, YlPXA2, and YlANT1 in presence of glucose and/or oleate. Cells were precultured in liquid YNB supplemented with 1% glucose and 0.5% yeast extract for 15 h at 28 °C (T0). Cells were then transferred to a fresh liquid YNB medium supplemented with 1% glucose, 3% oleate, or both 1% glucose and 3% oleate and incubated for 2 or 6 h at 28 °C. The expression profiles of Actin and ALG9 were used as endogenous controls for all the conditions tested. RT- and gDNA served as the negative and positive controls, respectively.

possibility that another protein is compensating for YlFaa1p and is able to activate FAs in cytoplasm, this result may suggest that unactivated FAs of varying chain length are being transported into the peroxisomes and activated in this organelle.

In conclusion, in contrast to what was seen in *S. cerevisiae*, activation takes place in the peroxisomes mainly for C6:0, C10:0 and DC18:1 and partially for C18:1. Additionally, all these results suggested that peroxisomes contain transporters of non-activated FAs as proposed above and activation of FA in peroxisome is a major way compares cytoplasmic FA activation.

3.5. Deleting YlANT1 from ΔYlpxa1 and ΔYlpxa2 had a synergistic effect on yeast growth on fatty acids

To decipher whether YlPxa1p and YlPxa2p work as homodimers or heterodimers, a double mutant—Δ*Ylpxa1* Δ*Ylpxa2*—was constructed

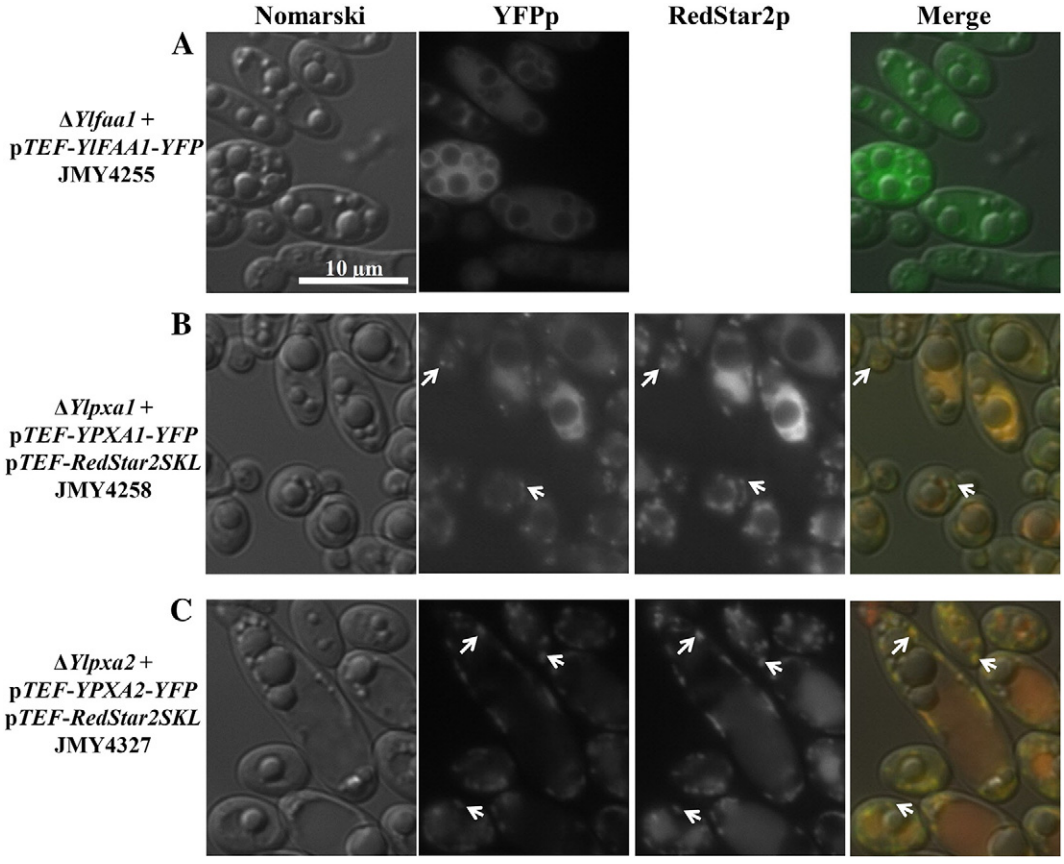

Fig. 4. Localization patterns of YlFaa1p, YlPxa1p, and YlPxa2p fused to YFP. The locations of (A) YlFaa1-YFPp, (B) YlPxa1-YFPp, and (C) YlPxa2-YFPp were determined after 24 h of growth on $YNBD_{0.5}O_3$. Peroxisomes were stained by a peroxisome-targeting fluorescent protein, RedStar2SKLp.

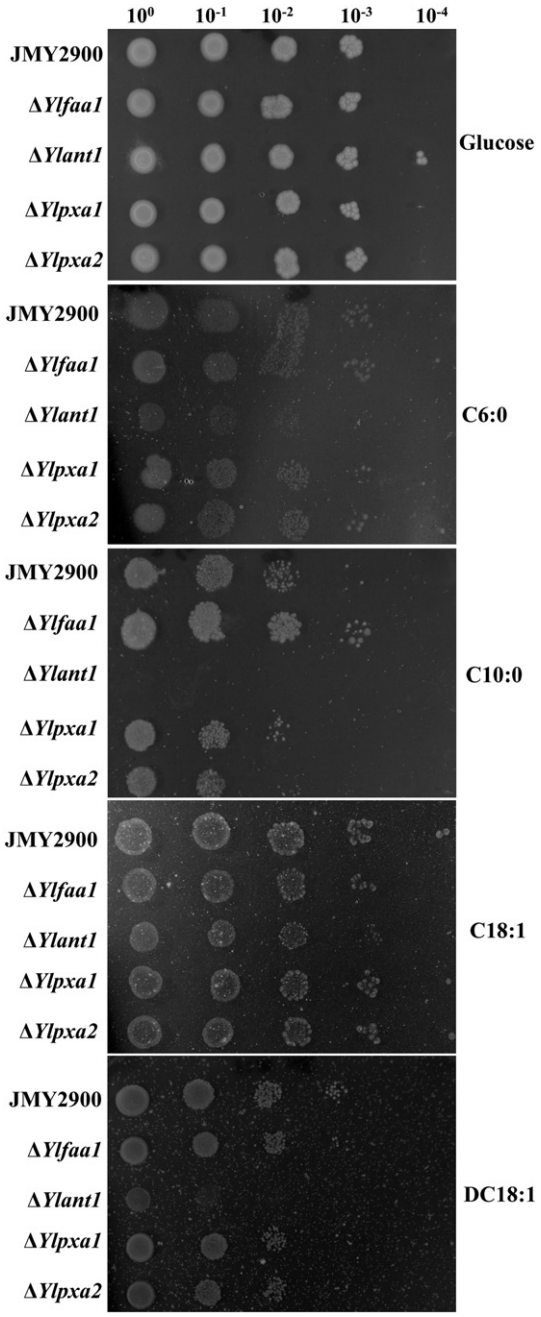

Fig. 5. Growth of the reference strain (JMY2900) and various mutants (Δ*Ylfaa1*, Δ*Ylant1*, Δ*Ylpxa1*, Δ*Ylpxa2*, and Δ*Ylpxa1* Δ*Ylpxa2*) on different carbon sources (0.2%). The following carbon sources were used: glucose; methyl caproate (C6:0); methyl decanoate (C10:0); oleate (C18:1); and octadecenedioic acid (DC18:1). Pictures were taken after 3 days of growth at 28 °C and show representative results from the three independent experiments.

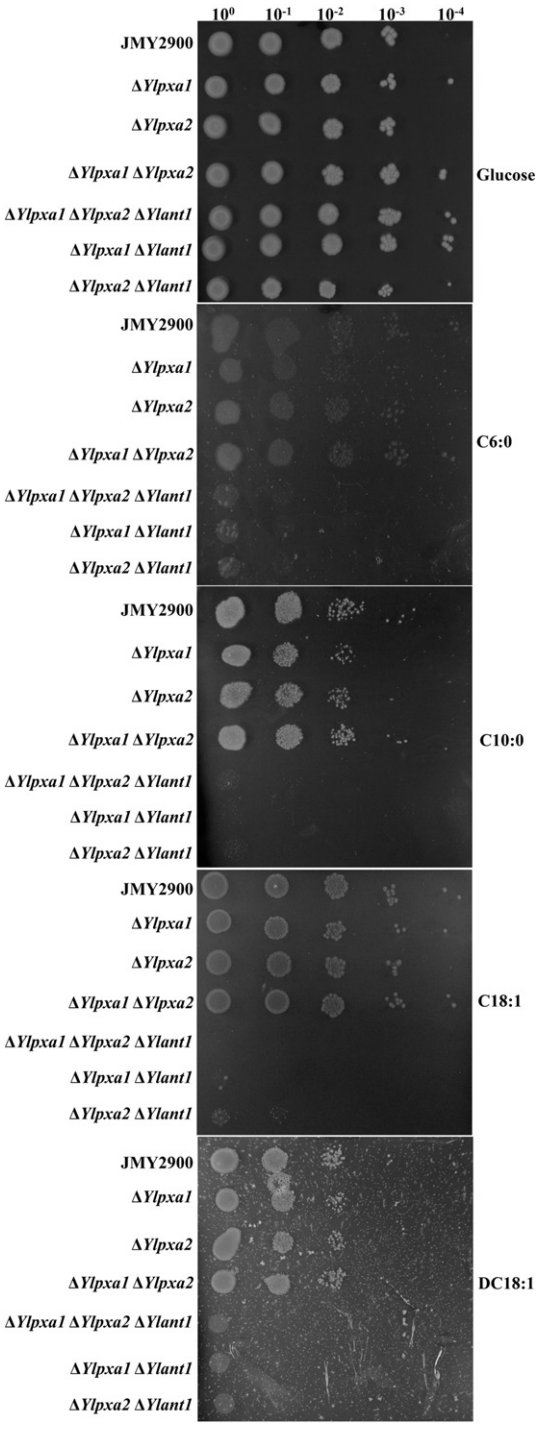

Fig. 6. Growth of JMY2900, Δ*Ylpxa1*, Δ*Ylpxa2*, Δ*Ylpxa1* Δ*Ylpxa2*, Δ*Ylpxa1* Δ*Ylant1*, Δ*Ylpxa2* Δ*Ylant1*, and Δ*Ylpxa1* Δ*Ylpxa2* Δ*Ylant1* on different carbon sources (0.2%). The carbon sources are the same as in Fig. 5. Pictures were taken after 3 days of growth at 28 °C and show representative results from the three independent experiments.

(JMY3159). Like the single mutants, Δ*Ylpxa1* Δ*Ylpxa2* was able to grow on C6:0, C10:0, C18:1 and DC18:1 (Fig. 6 and Fig. S1C). This result confirms that FAs are mainly being activated in the peroxisomes, unless another transporter is compensating for the absence of YlPxa1p/YlPxa2p. If YlPxa1p and YlPxa2p are exclusively responsible for the transport of activated FAs into the peroxisomes, then the deletion of *YlANT1* from the Δ*Ylpxa1* and Δ*Ylpxa2* mutants would be predicted to drastically decrease the mutants' ability to grow on FAs. To test this hypothesis, two double mutants—Δ*Ylpxa1* Δ*Ylant1* (JMY3797) and Δ*Ylpxa2* Δ*Ylant1* (JMY3811)—and a triple mutant—Δ*Ylpxa1* Δ*Ylpxa2* Δ*Ylant1* (JMY3795)—were constructed. As expected, synergic effect of these mutations was observed, especially for C18:1 since growth on FAs was strongly affected for all three mutants (Fig. 6 compare Fig. 5 and Fig. S1D). Since similar results were obtained with these mutants, this strongly suggests that YlPxa1p and Ylpxa2p may function as heterodimer as their homologue in *S. cerevisiae* [19,52].

3.6. YlFaa1p is the only cytoplasmic acyl-CoA synthetase in Y. lipolytica

To determine if there are other proteins that YlFaa1p could activate cytoplasmic FAs, we constructed a strain devoid of *YlANT1* and *YlFAA1*

(JMY3464). If YlFaa1p is the only cytoplasmic acyl-CoA synthetase, this strain should not grow on FAs since no activation of FA is possible in this strain. No growth was observed on C6:0, C10:0, C18:1, and DC18:1 (Fig. 7), showing that *Y. lipolytica* has only one cytoplasmic acyl-CoA synthetase, YlFaa1p.

3.7. In Y. lipolytica, decreased uptake of FAs into the peroxisomes leads to increased lipid accumulation

Y. lipolytica is an oleaginous yeast that is able to accumulate lipids in lipid bodies. Strains in which β-oxidation has been impaired—such as strains whose acyl CoA oxidases have been eliminated (Pox1-6p; enzymes involved in FA degradation, [33])—or strains in which remobilization processes have been affected—such as Δ*Ylfat1* [12] or Δ*tgl4* [10,11]—accumulate greater quantities of lipids than do wild type strains. To analyze the impact of deleting *YlANT1*, *YlFAA1*, *YlPXA1*, and *YlPXA2* on lipid accumulation, we performed a set of experiments in which we grew mutants in a medium that favors lipid accumulation, $YNBD_{0.5}O_3$. Fluorescent staining of lipids clearly showed that all the mutants from

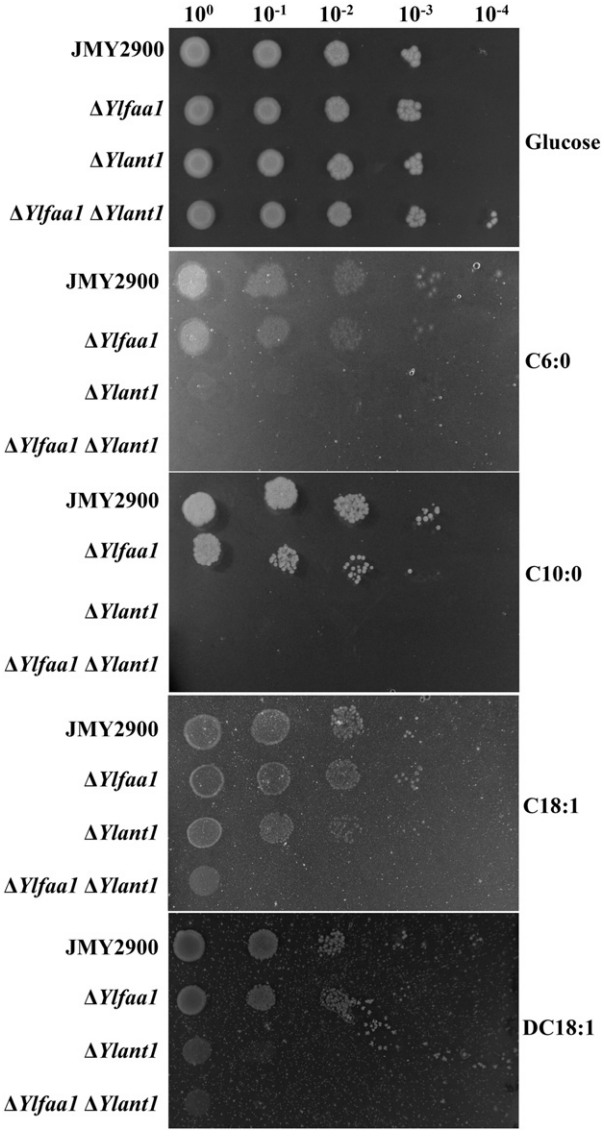

Fig. 7. Growth of JMY2900, Δ*Ylfaa1*, Δ*Ylant1*, and Δ*Ylfaa1* Δ*Ylant1* on various carbon sources (0.2%). The carbon sources are the same as in Fig. 5. Pictures were taken after 3 days of growth at 28 °C and show representative results from the three independent experiments.

which *YlPXA1* and *YlPXA2* had been deleted contained larger lipid bodies than did the reference strain, JMY2900 (Fig. 8D, E, F, H, I, J, L and M vs. Fig. 8A). Moreover, the deletion of *YlANT1* increased the number and size of lipid bodies only when *YlPXA1* and/or *YlPXA2* had also been deleted; in such mutants, lipid bodies filled most of the cell (Fig. 8H, I, J, M vs. Fig. 8A and B). Moreover, although the viability of the Δ*Ylpxa1* Δ*Ylpxa2* and Δ*Ylant1* mutants was similar to that of JMY2900 (99.3% survival) in $YNBD_{0.5}O_3$ (data not shown), the viability of the Δ*Ylpxa1* Δ*Ylpxa2* Δ*Ylant1* mutant was severely affected since only 50% of its cells survived 24 h of culture (Fig. 8J and Fig. S2). The loss of viability in the Δ*Ylpxa1* Δ*Ylpxa2* Δ*Ylant1* mutant was unexpected and may be linked to a deregulation of lipid homeostasis. Interestingly, there was a synergistic effect when *YlFAT1* was deleted at the same time as *YlPXA1* and *YlPXA2*—more and larger lipid bodies were observed in the triple mutant (Fig. 8L and M vs. Fig. 8J).

In order to confirm that greater lipid body size and number was correlated with a higher level of lipid accumulation, gas chromatography was carried out on all the mutants. Indeed, while lipid accumulation attained 24% of CDW in JMY2900, accumulation levels were around 35–37% of CDW in Δ*Ylpxa1* and/or Δ*Ylpxa2* and reached 42–53% of CDW in Δ*Ylpxa1* and Δ*Ylpxa2* strains from which *YlANT1* and/or *YlFAT1* had also been deleted (Fig. 9).

We wish to underscore that the deletion of *YlFAA1* strongly reduced lipid accumulation (Figs. 8C and 9), which demonstrates that, in *Y. lipolytica*, cytoplasmic activation is a necessary step in the storage of exogenous FAs in lipid bodies. In the Δ*Ylfaa1* mutant, lipid accumulation only reached about 8% of CDW, which corresponds to FA neosynthesis. In addition, the morphology of the Δ*Ylant1* Δ*Ylfaa1* mutant indicates that most of its cells died (Fig. 8G): CFU analysis confirmed that about 95% of the cells died after 24 h of culture in the $YNBD_{0.5}O_3$ medium (data not shown). This result explains why the cells did not grow on FAs—at least in the case of C18:1: a toxic effect manifested itself in this mutant because its cells were unable to activate the FAs. Therefore, the vulnerability of the Δ*Ylant1* Δ*Ylfaa1* mutant to FAs may explain the excess of free fatty acids (FFAs) in its cytoplasm. Indeed, Δ*Ylant1* Δ*Ylfaa1* accumulated (without any visible lipid bodies) slightly more lipids than did JMY2900 (31% vs. 24%; Fig. 9). However, as just explained, this result could stem from the presence of FFAs.

All these results suggest that FAs activated by YlFaa1p are partially stored in lipid bodies. Moreover, when FAs cannot rapidly enter peroxisomes (i.e., in the case of the Δ*Ylpxa1*, Δ*Ylpxa2* mutants), they are directed toward the storage pathway. It is unlikely that the second pathway, in which unactivated FAs enter the peroxisomes, could handle all the FAs coming into the cell under such conditions. This issue could explain why the Δ*Ylant1* mutant accumulated lipids at only slightly higher levels than did JMY2900 (Fig. 9). Additionally, when the entry of the activated FAs into the peroxisomes (as in the Δ*Ylpxa1* and/or Δ*Ylpxa2* mutants) and peroxisomal activation (in the Δ*Ylant1* mutant) are impaired, FAs are activated by YlFaa1p in the cytoplasm and stored in lipid bodies in the form of TAGs, which could explain why the Δ*Ylpxa1* Δ*Ylpxa2* Δ*Ylant1* mutant overaccumulated lipids. The phenotype demonstrated by strains from which *YlPXA1* and *YlPXA2* had been deleted was very similar to what is observed in individuals afflicted with X-linked adrenoleukodystrophy: this disease is characterized by the increased accumulation of lipids. The only difference between the Δ*Ylpxa1* and Δ*Ylpxa2* mutants and the Δ*ABCD1* mutant is the kind of FAs being accumulated: it is LCFAs (C18:1) in *Y. lipolytica* and very-long-chain fatty acids (C24:0, C26:0, and C26:1) in humans [24,34,34]. Moreover, lipid accumulation is one of the multiple phenotypes associated with the deletion of CTS (equivalent to ABCD1) in *Arabidopsis thaliana* [16].

3.8. β-oxidation is disturbed in mutant affecting in peroxisomal FA entrance

Previous work by our research group has shown that the FAs accumulated in *Y. lipolytica* grown on $YNBD_{0,5}O_3$ are a reflection of the FAs

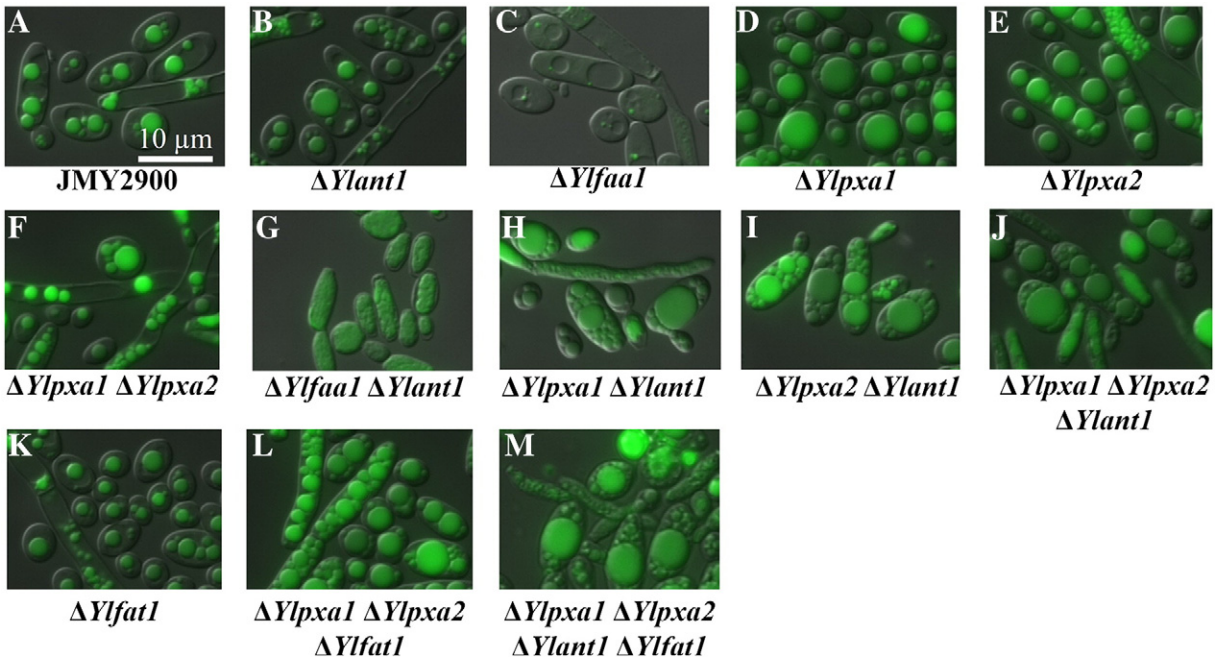

Fig. 8. Morphologies of the different strains after 24 h of culture in $YNBD_{0.5}O_3$. (A) JMY2900; (B) Δ*Ylant1* (JMY3237); (C) Δ*Ylfaa1* (JMY3234); (D) Δ*Ylpxa1* (JMY3230); (E) Δ*Ylpxa1* (JMY3233); (F) Δ*Ylpxa1* Δ*Ylpxa2* (JMY3159); (G) Δ*Ylant1* Δ*Ylfaa1* (JMY3464); (H) Δ*Ylpxa1* Δ*Ylant1* (JMY3797); (I) Δ*Ylpxa2* Δ*Ylant1* (JMY3811); (J) Δ*Ylpxa1* Δ*Ylpxa2* Δ*Ylant1* (JMY3795); (K) Δ*Ylfat1* (JMY3240); (L) Δ*Ylpxa1* Δ*Ylpxa2* Δ*Ylfat1* (JMY4160); and (M) Δ*Ylpxa1* Δ*Ylpxa2* Δ*Ylant1* Δ*Ylfat1* (JMY4138). TAG fluorescence was obtained by staining cells for neutral lipids with BodiPy® stain.

present in the medium [3]. The oleic acid used in this study was 73% C18:1(n−9), 7% C18:2(n−6), 4.7% C16:1(n−7), 3.9% C16:0, 0.9% C16:1(n−9), and 0.7% C18:0. Interestingly, most of the mutants had FA profiles that differed from that of the reference strain, JMY2900, especially for C16:0, C16:1(n−7), C16:1(n−9), C18:0 and C18:1 (Fig. 10). No significative difference was observed for C18:2, with 10% of FA for all the studied strains. The Δ*Ylfaa1* mutant contained 3-, 3.3-, and 2-fold more C16:0, C16:1(n−9), and C18:0, respectively, than the reference strain (Fig. 10A, B, C). However, it contained only 4.7% C16:1(n−7) and 60% C18:1(n−9); these values were 8% and 68%, respectively, for JMY2900. C16:1(n−9) cannot be synthesized by cells and derives essentially from the degradation of any C18:1(n−9) present in the medium. The overrepresentation of C16:1(n−9) in the Δ*Ylfaa1* mutant may indicate that it had higher levels of β-oxidation than did the reference strain. This explanation also fits well with the lower levels of C18:1(n−9) observed in this mutant as compared to JMY2900; FAs may not accumulate in the mutant, resulting in more accessible FAs for β-oxidation. Although these results were obtained under different conditions than those of [58] (use of oleate vs. YPD media, respectively), both sets of findings show that the deletion of *YlFAA1* can increase the production of C16 FAs and saturated FAs.

Δ*Ylpxa1*, Δ*Ylpxa2*, and Δ*Ylpxa1* Δ*Ylpxa2* accumulated 2.5-fold less C16:1(n−9), 2-fold less C18:0, and 1.5-fold less C16:1(n−7) than did JMY2900 (Fig. 10B, C). They also accumulated more C18:1(n−9) than did JMY2900 (around 75–77% vs. 68%; Fig. 10D). All together, these results suggest that, as previously shown for YlFat1p ([12]; Fig. 9B), Δ*Ylpxa1* and/or Δ*Ylpxa2* are worse at degrading C18:1(n−9). Furthermore, these data confirm that YlPxa1p and YlPxa2p transport C18:1

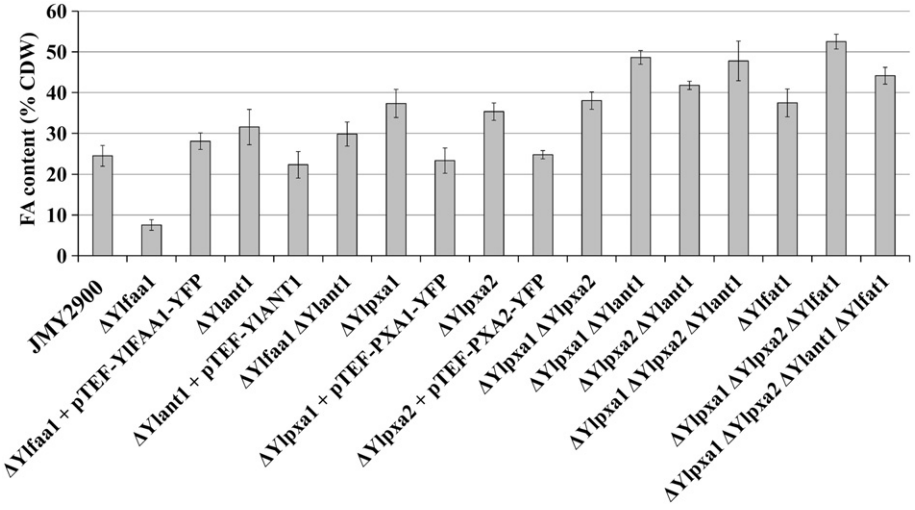

Fig. 9. FA content of various strains cultivated on $YNBD_{0.5}O_3$. Cells were grown for 24 h on $YNBD_{0.5}O_3$. These results are the mean values ± SD from the three independent replicates. Lipids were extracted using the procedure described in [7], and FA content was determined using gas chromatography. CDW = cell dry weight.

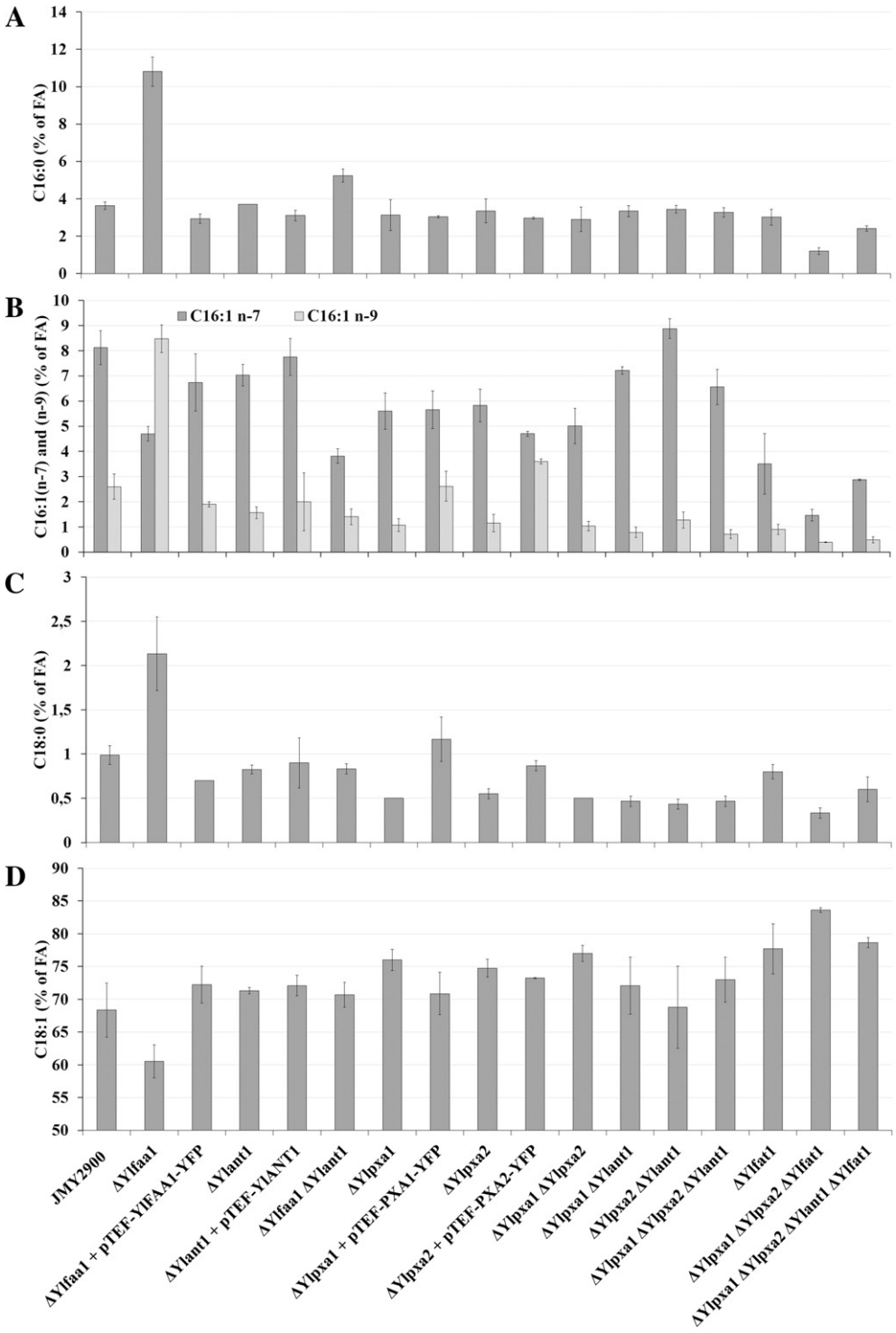

Fig. 10. FA profiles of various strains, expressed as percentages of total FA. (A) C16:0; (B) C16:1(n−7) and C16:1(n−9); (C) C18:0; and (D) C18:1(n−9).

(n−9) into the peroxisomes. Interestingly, Δ*Ylpxa1* Δ*Ylpxa2* Δ*Ylfat1* displayed a more dramatic phenotype. Indeed, compared to JMY2900, this triple mutant contained 3-fold less C16:0, 6-fold less C16:1(n−9), 5.5−fold less C16:1(n−7), and 3-fold less C18:0 and accumulated up to 84% of CDW of C18:1(n−9) (Fig. 10). Finally, FA degradation was altered in this triple mutant because the inactivation of *YlPXA1* and *YlPXA2* reduced the entry of activated FAs into the peroxisomes and the inactivation of *YlFAT1* reduced the remobilization of FAs stored as TAGs in the lipid bodies [12]. Surprisingly, the deletion of *YlANT1* from the wild-type background only weakly affected FA composition. However, when this same gene was deleted from the Δ*Ylfaa1* background, levels of C16:0 were increased 1.5-fold whereas levels of C16:1(n−7) and C16:1(n−9) were reduced 2-fold (Fig. 10). For some unknown reason, when *YlANT1* was deleted from the Δ*Ylpxa1*, and/or Δ*Ylpxa2*, or Δ*Ylpxa1* Δ*Ylpxa2* Δ*Ylfat1* backgrounds, levels of C16:1(n−7) increased.

3.9. Remobilization is blocked in the ΔYlpxa1 ΔYlpxa2 ΔYlfat1 mutant

When *Y. lipolytica* lacks carbon, stored lipids are remobilized. To determine if one of the genes of interest is involved in this process,

lipid remobilization was examined in the different mutants. Cells were cultivated in a medium that favored accumulation ($YNBD_{0,5}O_3$), washed, and then transferred to $YNBC_0$, a medium without a carbon source. Lipid remobilization was quantified using gas chromatography (Fig. 11). As observed by [12], the reference strain, JMY2900, rapidly remobilized lipids (Fig. 11A). Strains from which *YlPXA1*, *YlPXA2*, *YlPXA1* and *YlPXA2*, or *YlANT1* had been deleted had the same remobilization profiles as JMY2900, which suggests that these genes are not involved in lipid remobilization or that other genes compensate for their absence (Fig. 11A). However, a slight decrease in lipid remobilization was observed when *YlANT1* was deleted from the Δ*Ylpxa1*, Δ*Ylpxa2*, and Δ*Ylpxa1* Δ*Ylpxa2* mutants (Fig. 11B). This result indicates that these genes work together to remobilize lipids but are part of two different pathways. Since remobilization still occurs in these mutants, a third lipid remobilization pathway may exist. This last pathway could be dependent on YlFat1p, which has been shown to be involved in lipid remobilization [12]. To determine which proteins are the most important in this process, we examined lipid remobilization in the Δ*Ylpxa1* Δ*Ylpxa2* Δ*Ylfat1* mutant (Fig. 11C). Surprisingly, lipid remobilization was completely absent from this strain. This result could explain why Δ*Ylpxa1* Δ*Ylpxa2* Δ*Ylfat1* accumulated a very high level of lipids in Fig. 8. This result shows that YlFat1p, YlPxa1p, and YlPxa2p are, together, essential for lipid remobilization. Furthermore, this result suggests that the YlAnt1p-dependent pathway is of minor importance and that most of the FAs released are activated by YlFaa1p in the cytoplasm before they enter the peroxisomes via the heterodimer YlPxa1p/YlPxa2p. We suggest that YlFat1p could be involved in the transport of FAs from the lipid bodies to the peroxisomes [12]; furthermore, Choi and Martin [63] showed that ScFat1p demonstrates acyl-CoA synthetase activity. This finding suggests that YlFat1p may able to activate FAs as they are being transferred between the lipid bodies and the peroxisomes, explaining also why YlAnt1p is not really important for remobilization.

4. Conclusion and perspectives

Until now, most studies concerning FA transport and activation have been performed in the model yeast species *S. cerevisae*. However, research has recently shown that lipid metabolism differs greatly among yeast species [11,12,59]. Therefore, it is impossible to make generalizations about lipid metabolism in yeasts; it cannot be assumed that what occurs in *S. cerevisiae* also occurs in other yeasts and, particularly, in oleaginous yeasts. Although our study species, *Y. lipolytica*, does possess FA transport and activation proteins that are similar to those of *S. cerevisiae* (Faa1p, Pxa1p, Pxa2p, Ant1p), we found that FA transport and activation is actually different in *Y. lipolytica* than in *S. cerevisiae*. In fact, our results suggest that other, unidentified proteins might play an important role in these processes. Fig. 12 depicts our proposed model for FA transport and activation in *Y. lipolytica*. External fatty acids (FA ex) enter cells via a single or multiple transporters that remain to be identified. Internal free FA (FA in) could bind to the fatty acid binding protein (FABP, ❶), activated by the cytoplasmic YlFaa1p (❷) or transported into peroxisomes (❸) with chain length preferences. Activated FAs can then be either stored

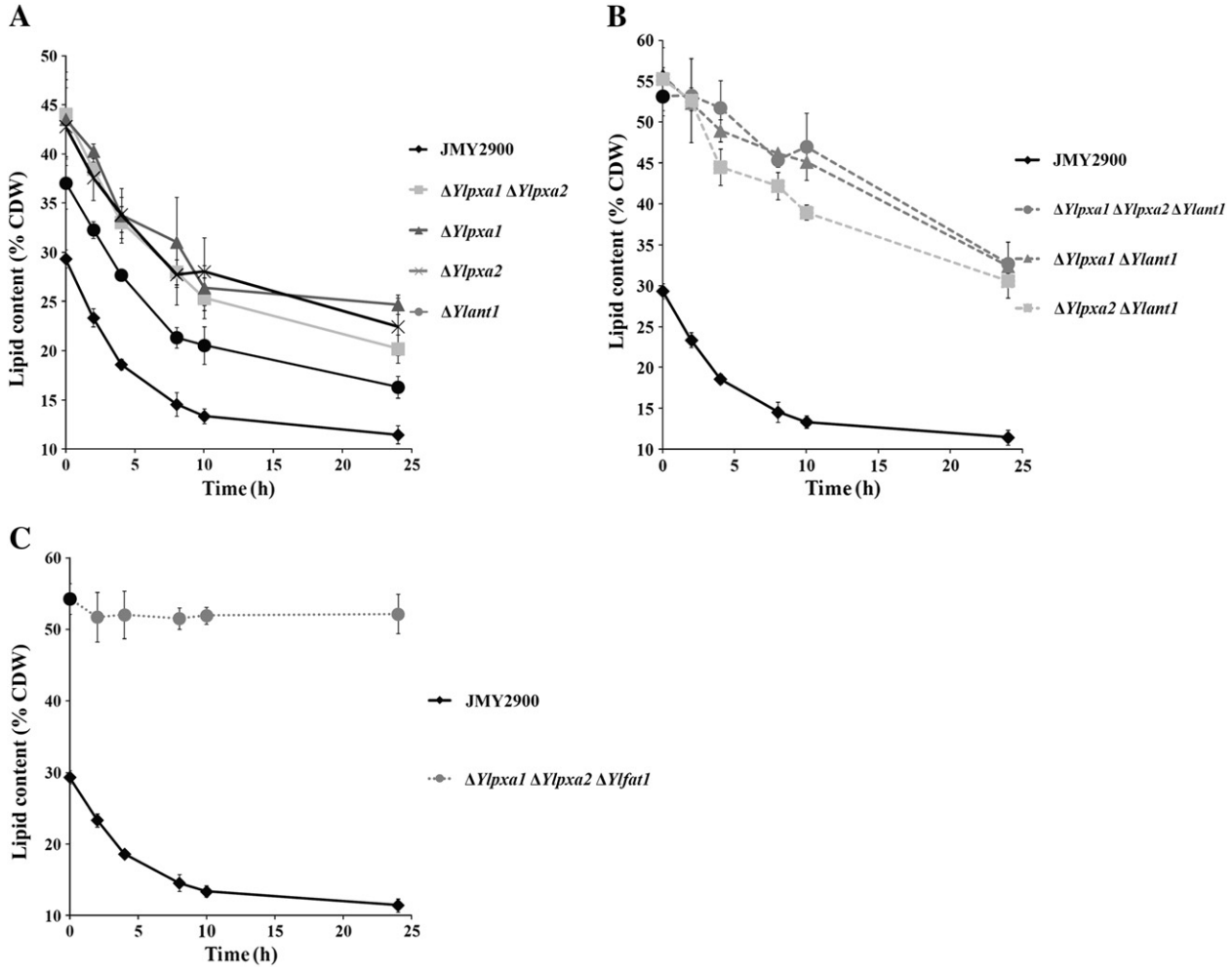

Fig. 11. Variation in FA content during lipid remobilization in various strains grown in $YNBC_0$ medium. Lipid remobilization in (A) JMY2900, Δ*Ylpxa1* Δ*Ylpxa2*, Δ*Ylpxa1*, Δ*Ylpxa2*, and Δ*Ylant1*; (B) JMY2900, Δ*Ylpxa1* Δ*Ylpxa2* Δ*Ylant1*, Δ*Ylpxa1* Δ*Ylant1*, and Δ*Ylpxa2* Δ*Ylant1*; (C) JMY2900 and Δ*Ylpxa1* Δ*Ylpxa2* Δ*Ylfat1*. CDW—cell dry weight.

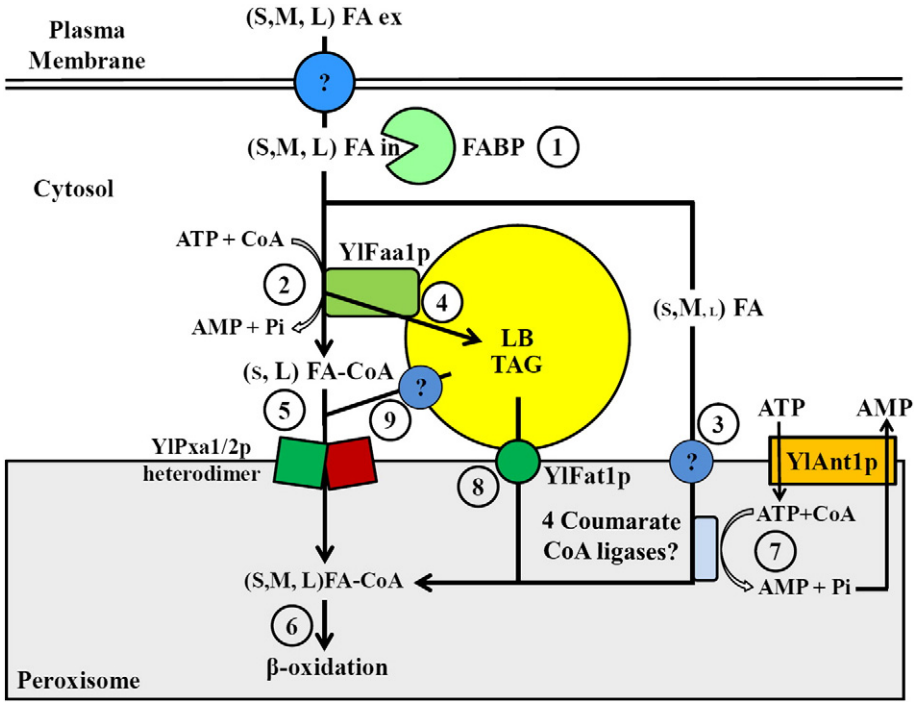

Fig. 12. Model of FA transport and activation in *Y. lipolytica*. LB, lipid body; (S, M, L) FA, short-, medium-, and long-chain fatty acids, (S, M, L) FA-CoA, short-, medium-, and long-chain activated fatty acids. The size of the S, M and L indicate the preferred pathways.

in lipid bodies as TAGs (small- and medium-chain FAs are stored after an elongation step) (❹) or they can enter peroxisomes via the heterodimer YlPxa1p/YlPxa2p (❺) and be degraded as a result of β-oxidation (❻). Unactivated FAs that enter peroxisomes via an unidentified transporter (❸) are activated by enzymes 4 coumarate CoA ligase (see below) that required ATP transported by YlAnt1p (❼) (note: this is the only pathway for MCFA such as C10:0). FAs from TAG are released from lipid bodies via two principal pathways: one involving YlFat1p (❽) and another one involving an unidentified pathway (❾).

Presence of free fatty acid in the cells has been the subject of extensive debate. Several lines of evidences suggest that they are, indeed, free fatty acid in *Y. lipolytica*. Thus, there is an increase amount of FFA in cells deleted for the six acyl-CoA oxidases (*pox1-6*Δ) and in cells deleted for the multifunctional enzyme *MFE2* (*mfe2*Δ) [10]. On the opposite, there is very small amount of FFA in wild-type and in cells deleted for the triglyceride lipases *TGL3* and *TGL4* (*tgl3*Δ, *tgl4*Δ and *tgl3*Δ *tgl4*Δ) during carbon starvation [11]. Several hypotheses could be postulated to escape to the FFA toxicity. One would be the presence of sterol carrier protein with fatty-acid and fatty-acyl-CoA binding activity [9,14], (Fig. 12). Another one would be the transport of long-chain fatty acids into the mitochondria in parallel to the YlPxa1p–YlPxa2p peroxisomal transporter pathway. Indeed, carnitine was shown to be involved for the transport of long-chain fatty acids into mitochondria in mammals [28].

In order to validate our proposed model we reconstructed a metabolic model using Raven toolbox [1] which was composed of 42 reactions and 15 metabolites localized in 4 different compartments (extracellular, cytoplasm, peroxisome and lipid body). This mathematical framework allowed us to make predictions, by using flux balance analysis, in the biomass and lipid bodies' formation capacities of different genetic backgrounds using different fatty acids as carbon sources. We therefore compared the predicted values with our experimental data (Table 3), which proved a high reliability of the proposed model, showing only four minor mismatches. These differences were all found in the ability to use C6:0 by mutants Δ*Ylant1*, which point out to an alternative pathway to degrade this fatty acids, that could be associated to mitochondria such as suggested in [18]. Additionally, this metabolic model can be included in the two previously published genome scale metabolic model of *Y. lipolytica* [32,39], which are not well defined in their pathways to transport and activate fatty acids. Hence, this will lead to the improvement of the accuracy of future predictions using any of the genome scale metabolic models.

Understanding how FAs can be activated in peroxisomes is of great interest. Until now, no proteins demonstrating such a function had been identified. However, the recent biochemical characterization of enzymes encoded by peroxisomal 4-coumarate:coenzyme A ligase-like genes shows that such proteins generally do not convert the substrates accepted by true 4-coumarate CoA ligase enzymes to the corresponding CoA esters [8,25]. Indeed, many accept fatty acyl substrates—such as 12-oxo-phytodienoic acid (OPDA) and OPDA derivatives (jasmonic acid precursors; [25,27])—and medium- to long-chain fatty acids [25,48]. For example, the product yielded by *At4g05160* is able to activate medium- and long-chain fatty acids, medium-chain fatty acids bearing phenyl substitutions, and jasmonic acid precursors (12-oxo-phytodienoic acid and 3-oxo-2-(2′-pentenyl)-cyclopentane-1-hexanoic acid). In contrast, the product yielded by *At5g63380* was only able to activate medium- and long-chain fatty acids and 12-oxo-phytodienoic acid [48]. We found that *Y. lipolytica* has 10 genes coding for putative 4-coumarate-CoA ligases-like that are potentially found in peroxisomes. These proteins could be equivalent in function to ScFaa2p in *S. cerevisiae*, and further research is needed to clarify FA peroxisomal activation in *Y. lipolytica*.

Supplementary data to this article can be found online at http://dx.doi.org/10.1016/j.bbalip.2015.04.004.

Acknowledgments

We thank the French vegetable oil and protein industry for their financial support in the form of the FIDOP/FASO Fund (Fonds d'action stratégique des oléagineux). We would also like to thank Thierry Dulermo for his helpful comments on the manuscript and Jessica Pearce and Lindsay Higgins for their language editing services.

Table 3
Comparison between mathematical model and experimental results.

Strain	Carbon source	Biomass		Lipid bodies	
		Experimental	Predicted	Experimental	Predicted
WT (JMY2900)	C18:1	●	●	●	●
	C10:0	●	●		
	C6:0	●	●		
Δ*Ylfaa1*	C18:1	●	●	○	○
	C10:0	●	●		
	C6:0	●	●		
Δ*Ylant1*	C18:1	●	●	●	●
	C10:0	○	○		
	C6:0	○/w	○		
ΔYlpxa1	C18:1	●	●	●	●
	C10:0	●	●		
	C6:0	●	●		
Δ*Ylpxa2*	C18:1	●	●	●	●
	C10:0	●	●		
	C6:0	●	●		
Δ*Ylpxa1*	C18:1	●	●	●	●
Δ*Ylpxa2*	C10:0	●	●		
	C6:0	●	●		
Δ*Ylpxa1*	C18:1	○	○	●	●
Δ*Ylpxa2*	C10:0	○	○		
Δ*Ylant1*	C6:0	○/w	○		
Δ*Ylpxa1*	C18:1	○	○	●	●
Δ*Ylant1*	C10:0	○	○		
	C6:0	○/w	○		
Δ*Ylpxa2*	C18:1	○	○	●	●
Δ*Ylant1*	C10:0	○	○		
	C6:0	○/w	○		
Δ*Ylfaa1*	C18:1	○	○	○	○
Δ*Ylant1*	C10:0	○	○		
	C6:0	○	○		
Δ*Ylfat1*	C18:1	●	●	●	●
	C10:0	●	●		
	C6:0	●	●		
Δ*Ylpxa1*	C18:1	●	●	●	●
Δ*Ylpxa2*	C10:0	●	●		
Δ*Ylfat1*	C6:0	●	●		
Δ*Ylpxa1*	C18:1	○	○	●	●
Δ*Ylpxa2*	C10:0	○	○		
Δ*Ylant1*	C6:0	○	○		
Δ*Ylfat1*					

The table shows the validation of the proposed model for activation and transport of fatty acids in *Yarrowia lipolytica* by comparing the predictions of the reconstructed mathematical model to the experimental results. Different backgrounds were tested for their capacity to grow in fatty acids C18:1, C10:0 or C6:0 both in vivo (Experimental data) and in silico (Predicted). Additionally, their ability to produce lipid bodies from external C18:1 was compared. ● growth/lipid bodies formation, ○ no growth/no lipid bodies formation, ○/w very weak growth or residual growth.

References

[1] R. Agren, L. Liu, S. Shoaie, W. Vongsangnak, I. Nookaew, J. Nielsen, The RAVEN toolbox and its use for generating a genome-scale metabolic model for *Penicillium chrysogenum*, PLoS Comput. Biol. 9 (2013) e1002980.

[2] G. Barth, C. Gaillardin, in: K. Wolf (Ed.), *Yarrowia lipolytica*, Non Conventional Yeasts in Biotechnology, vol. 1, Springer, Berlin, Germany 1996, pp. 313–388.

[3] A. Beopoulos, Z. Mrozova, F. Thevenieau, M.T. Le Dall, I. Hapala, S. Papanikolaou, T. Chardot, J.M. Nicaud, Control of lipid accumulation in the yeast *Yarrowia lipolytica*, Appl. Environ. Microbiol. 74 (2008) 7779–7789.

[4] A. Beopoulos, J. Cescut, R. Haddouche, J.L. Uribelarrea, C. Molina-Jouve, J.M. Nicaud, *Yarrowia lipolytica* as a model for bio-oil production, Prog. Lipid Res. 48 (2009) 375–387.

[5] A. Beopoulos, J.M. Nicaud, C. Gaillardin, An overview of lipid metabolism in yeasts and its impact on biotechnological processes, Appl. Microbiol. Biotechnol. 90 (2011) 1193–1206.

[6] P.N. Black, C.C. DiRusso, Yeast acyl-CoA synthetases at the crossroads of fatty acid metabolism and regulation, Biochim. Biophys. Acta 1771 (2007) 286–298.

[7] J. Browse, P.J. McCourt, C.R. Somerville, Fatty acid composition of leaf lipids determined after combined digestion and fatty acid methyl ester formation from fresh tissue, Anal. Biochem. 152 (1986) 141–145.

[8] M.A. Costa, D.L. Bedgar, S.G. Moinuddin, K.W. Kim, C.L. Cardenas, F.C. Cochrane, J.M. Shockey, G.L. Helms, Y. Amakura, H. Takahashi, J.K. Milhollan, L.B. Davin, J. Browse, N.G. Lewis, Characterization in vitro and in vivo of the putative multigene 4-coumarate:CoA ligase network in *Arabidopsis*: syringyl lignin and sinapate/sinapyl alcohol derivative formation, Phytochemistry 66 (2005) 2072–2091.

[9] E.C. Dell'Angelica, M.R. Ermacora, J.A. Santome, Purification and partial characterization of a fatty acid-binding protein from the yeast, *Yarrowia lipolytica*, Biochem. Mol. Biol. Int. 39 (1996) 439–445.

[10] T. Dulermo, J.M. Nicaud, Involvement of the G3P shuttle and β-oxidation pathway in the control of TAG synthesis and lipid accumulation in *Yarrowia lipolytica*, Metab. Eng. 13 (2011) 482–491.

[11] T. Dulermo, B. Tréton, A. Beopoulos, A.P. Kabran Gnankon, R. Haddouche, J.M. Nicaud, Characterization of the two intracellular lipases of *Y. lipolytica* encoded by *TGL3* and *TGL4* genes: new insights into the role of intracellular lipases and lipid body organization, Biochim. Biophys. Acta 1831 (2013) 1486–1495.

[12] R. Dulermo, H. Gamboa-Meléndez, T. Dulermo, F. Thevenieau, J.M. Nicaud, The fatty acid transport protein Fat1p is involved in the export of fatty acids from lipid bodies in *Yarrowia lipolytica*, FEMS Yeast Res. 14 (2014) 883–896.

[13] R.J. Duronio, L.J. Knoll, J.I. Gordon, Isolation of a *Saccharomyces cerevisiae* long chain fatty acyl:CoA synthetase gene (FAA1) and assessment of its role in protein N-myristoylation, J. Cell Biol. 117 (1992) 515–529.

[14] R.G. Ferreyra, N.I. Burgardt, D. Milikowski, G. Melen, A.R. Kornblihtt, E.C. Dell' Angelica, J.A. Santome, M.R. Ermacora, A yeast sterol carrier protein with fatty-acid and fatty-acyl-CoA binding activity, Arch. Biochem. Biophys. 453 (2006) 197–206.

[15] P. Fickers, M.T. Le Dall, C. Gaillardin, P. Thonart, J.M. Nicaud, New disruption cassettes for rapid gene disruption and marker rescue in the yeast *Yarrowia lipolytica*, J. Microbiol. Methods 55 (2003) 727–737.

[16] S. Footitt, S.P. Slocombe, V. Larner, S. Kurup, Y. Wu, T. Larson, I. Graham, A. Baker, M. Holdsworth, Control of germination and lipid mobilization by COMATOSE, the Arabidopsis homologue of human ALDP, EMBO J. 21 (2002) 2912–2922.

[17] M. Gatter, A. Förster, K. Bär, M. Winter, C. Otto, P. Petzsch, M. Ježková, K. Bahr, M. Pfeiffer, F. Matthäus, G. Barth, A newly identified fatty alcohol oxidase gene is mainly responsible for the oxidation of long-chain ω-hydroxy fatty acids in *Yarrowia lipolytica*, FEMS Yeast Res. 14 (2014) 858–872.

[18] R. Haddouche, S. Delessert, J. Sabirova, C. Neuvéglise, Y. Poirier, J.M. Nicaud, Roles of multiple acyl-CoA oxidases in the routing of carbon flow towards β-oxidation and polyhydroxyalkanoate biosynthesis in *Yarrowia lipolytica*, FEMS Yeast Res. 10 (2010) 917–927.

[19] E.H. Hettema, C.W. van Roermund, B. Distel, M. van den Berg, C. Vilela, C. Rodrigues-Pousada, R.J. Wanders, H.F. Tabak, The ABC transporter proteins Pat1 and Pat2 are required for import of long-chain fatty acids into peroxisomes of *Saccharomyces cerevisiae*, EMBO J. 15 (1996) 3813–3822.

[20] D.R. Johnson, L.J. Knoll, N. Rowley, J.I. Gordon, Genetic analysis of the role of *Saccharomyces cerevisiae* acyl-CoA synthetase genes in regulating protein N-myristoylation, J. Biol. Chem. 269 (1994) 18037–18046.

[21] D.R. Johnson, L.J. Knoll, D.E. Levin, J.I. Gordon, *Saccharomyces cerevisiae* contains four fatty acid activation (*FAA*) genes: an assessment of their role in regulating protein N-myristoylation and cellular lipid metabolism, J. Cell Biol. 127 (1994) 751–762.

[22] M. Garcia-Albornoz, S. Thankaswamy-Kosalai, A. Nilsson, L. Väremo, I. Nookaew, J. Nielsen, BioMet Toolbox 2.0: genome-wide analysis of metabolism and omics data, Nucleic Acids Res. 42 (2014) W175–W181.

[23] P. Kabran, T. Rossignol, C. Gaillardin, J.M. Nicaud, C. Neuvéglise, Alternative splicing regulates targeting of malate dehydrogenase in *Yarrowia lipolytica*, DNA Res. 19 (2012) 231–244.

[24] S. Kemp, R.J. Wanders, X-linked adrenoleukodystrophy: very long-chain fatty acid metabolism, ABC half-transporters and the complicated route to treatment, Mol. Genet. Metab. 90 (2007) 268–276.

[25] L. Kienow, K. Schneider, M. Bartsch, H.P. Stuible, H. Weng, O. Miersch, C. Wasternack, E. Kombrink, Jasmonates meet fatty acids: functional analysis of a new acyl-coenzyme A synthetase family from *Arabidopsis thaliana*, J. Exp. Bot. 59 (2008) 403–419.

[26] L.J. Knoll, D.R. Johnson, J.I. Gordon, Complementation of *Saccharomyces cerevisiae* strains containing fatty acid activation gene (*FAA*) deletions with a mammalian acyl-CoA synthetase, J. Biol. Chem. 270 (1995) 10861–10867.

[27] A.J. Koo, H.S. Chung, Y. Kobayashi, G.A. Howe, Identification of a peroxisomal acyl-activating enzyme involved in the biosynthesis of jasmonic acid in Arabidopsis, J. Biol. Chem. 281 (2006) 33511–33520.

[28] S. Kumaran, B. Deepak, B. Naveen, C. Panneerselvam, Effects of levocarnitine on mitochondrial antioxidant systems and oxidative stress in aged rats, Drugs R. D. 4 (2003) 141–147.

[29] F.M. Lasorsa, P. Scarcia, R. Erdmann, F. Palmieri, H. Rottensteiner, L. Palmieri, The yeast peroxisomal adenine nucleotide transporter: characterization of two transport modes and involvement in DeltapH formation across peroxisomal membranes, Biochem. J. 381 (2004) 581–585.

[30] M.T. Le Dall, J.M. Nicaud, C. Gaillardin, Multiple-copy integration in the yeast *Yarrowia lipolytica*, Curr. Genet. 26 (1994) 38–44.

[31] L.X. Liu, K. Janvier, V. Berteaux-Lecellier, N. Cartier, R. Benarous, P. Aubourg, Homo- and heterodimerization of peroxisomal ATP-binding cassette half-transporters, J. Biol. Chem. 274 (1999) 32738–32743.

[32] N. Loira, T. Dulermo, J.M. Nicaud, D.J. Sherman, A genome-scale metabolic model of the lipid-accumulating yeast *Yarrowia lipolytica*, BMC Syst. Biol. 6 (2012) 35.

[33] K. Mlíčková, E. Roux, K. Athenstaedt, S. d'Andrea, G. Daum, T. Chardot, J.M. Nicaud, Lipid accumulation, lipid body formation, and acyl coenzyme A oxidases of the yeast *Yarrowia lipolytica*, Appl. Environ. Microbiol. 70 (2004) 3918–3924.

[34] M. Morita, T. Imanaka, Peroxisomal ABC transporters: structure, function and role in disease, Biochim. Biophys. Acta 1822 (2012) 1387–1396.

[35] S. Müller, T. Sandal, P. Kamp-Hansen, H. Dalbøge, Comparison of expression systems in the yeasts *Saccharomyces cerevisiae*, *Hansenula polymorpha*, *Klyveromyces lactis*, *Schizosaccharomyces pombe* and *Yarrowia lipolytica*. Cloning of two novel promoters from *Yarrowia lipolytica*, Yeast 14 (1998) 1267–1283.

[36] K. Natter, P. Leitner, A. Faschinger, H. Wolinski, S. McCraith, S. Fields, S.D. Kohlwein, The spatial organization of lipid synthesis in the yeast *Saccharomyces cerevisiae* derived from large scale green fluorescent protein tagging and high resolution microscopy, Mol. Cell. Proteomics 4 (2005) 662–672.
[37] J.M. Nicaud, C. Madzak, P. van den Broek, C. Gysler, P. Duboc, P. Niederberger, C. Gaillardin, Protein expression and secretion in the yeast *Yarrowia lipolytica*, FEMS Yeast Res. 2 (2002) 371–379.
[38] L. Palmieri, H. Rottensteiner, W. Girzalsky, P. Scarcia, F. Palmieri, R. Erdmann, Identification and functional reconstitution of the yeast peroxisomal adenine nucleotide transporter, EMBO J. 20 (2001) 5049–5059.
[39] P. Pan, Q. Hua, Reconstruction and in silico analysis of metabolic network for an oleaginous yeast, *Yarrowia lipolytica*, PLoS One 7 (2012) e51535.
[40] A. Querol, E. Barrio, T. Huerta, D. Ramón, Molecular monitoring of wine fermentations conducted by active dry yeast strains, Appl. Environ. Microbiol. 58 (1992) 2948–2953.
[41] C.W. van Roermund, R. Drissen, M. van Den Berg, L. Ijlst, E.H. Hettema, H.F. Tabak, H.R. Waterham, R.J. Wanders, Identification of a peroxisomal ATP carrier required for medium-chain fatty acid β-oxidation and normal peroxisome proliferation in *Saccharomyces cerevisiae*, Mol. Cell. Biol. 21 (2001) 4321–4329.
[42] C.W. van Roermund, W.F. Visser, L. Ijlst, A. van Cruchten, M. Boek, W. Kulik, H.R. Waterham, R.J. Wanders, The human peroxisomal ABC half transporter ALDP functions as a homodimer and accepts acyl-CoA esters, FASEB J. 22 (2008) 4201–4208.
[43] C.W. van Roermund, W.F. Visser, L. Ijlst, H.R. Waterham, R.J. Wanders, Differential substrate specificities of human ABCD1 and ABCD2 in peroxisomal fatty acid β-oxidation, Biochim. Biophys. Acta 1811 (2011) 148–152.
[44] C.W. van Roermund, L. Ijlst, W. Majczak, H.R. Waterham, H. Folkerts, R.J. Wanders, K.J. Hellingwerf, Peroxisomal fatty acid uptake mechanism in *Saccharomyces cerevisiae*, J. Biol. Chem. 287 (2012) 20144–20153.
[45] H. Rottensteiner, L. Palmieri, A. Hartig, B. Hamilton, H. Ruis, R. Erdmann, A. Gurvitz, The peroxisomal transporter gene ANT1 is regulated by a deviant oleate response element (ORE): characterization of the signal for fatty acid induction, Biochem. J. 365 (2002) 109–117.
[46] Y. Sakai, A. Saiganji, H. Yurimoto, K. Takabe, H. Saiki, N. Kato, The absence of Pmp47, a putative yeast peroxisomal transporter, causes a defect in transport and folding of a specific matrix enzyme, J. Cell Biol. 134 (1996) 37–51.
[47] J. Sambrook, T. Maniatis, E.F. Fritsch, Molecular Cloning: A Laboratory Manual, 2nd edn Cold Spring Harbor Laboratory Press, Cold Spring Harbor, New York, 1989.
[48] K. Schneider, L. Kienow, E. Schmelzer, T. Colby, M. Bartsch, O. Miersch, C. Wasternack, E. Kombrink, H.P. Stuible, A new type of peroxisomal acyl-coenzyme A synthetase from *Arabidopsis thaliana* has the catalytic capacity to activate biosynthetic precursors of jasmonic acid, J. Biol. Chem. 280 (2005) 13962–13972.
[49] N. Shani, D. Valle, A *Saccharomyces cerevisiae* homolog of the human adrenoleukodystrophy transporter is a heterodimer of two half ATP-binding cassette transporters, Proc. Natl. Acad. Sci. U. S. A. 93 (1996) 11901–11906.
[50] M.S. Smit, M.M. Mokgoro, E. Setati, J.M. Nicaud, alpha, omega-Dicarboxylic acid accumulation by acyl-CoA oxidase deficient mutants of *Yarrowia lipolytica*, Biotechnol. Lett. 27 (2005) 859–864.
[51] J.J. Smith, M. Marelli, R.H. Christmas, F.J. Vizeacoumar, D.J. Dilworth, T. Ideker, T. Galitski, K. Dimitrov, R.A. Rachubinski, J.D. Aitchison, Transcriptome profiling to identify genes involved in peroxisome assembly and function, J. Cell Biol. 158 (2002) 259–271.
[52] E.E. Swartzman, M.N. Viswanathan, J. Thorner, The *PAL1* gene product is a peroxisomal ATP-binding cassette transporter in the yeast *Saccharomyces cerevisiae*, J. Cell Biol. 132 (1996) 549–563.
[53] F. Thevenieau, Metabolic engineering of the yeast *Yarrowia lipolytica* for the production of long-chain dicarboxylic acids from renewable oil feedstock, Institut National Agronomique Paris-Grignon, France, 2006. (PhD thesis).
[54] F. Thevenieau, M.T. Le Dall, B. Nthangeni, S. Mauersberger, R. Marchal, J.M. Nicaud, Characterization of *Yarrowia lipolytica* mutants affected in hydrophobic substrate utilization, Fungal Genet. Biol. 44 (2007) 531–542.
[55] F. Thevenieau, A. Beopoulos, T. Desfougeres, J. Sabirova, K. Albertin, S. Zinjarde, J.M. Nicaud, Uptake and assimilation of hydrophobic substrates by the oleaginous yeast *Yarrowia lipolytica*, in: K.N. Timmis (Ed.), Handbook of Hydrocarbon and Lipid Microbiology, Springer, ISBN: 978-3-540-77584-3 2010, pp. 1514–1525.
[56] A. Tzagoloff, J. Jang, D.M. Glerum, M. Wu, *FLX1* codes for a carrier protein involved in maintaining a proper balance of flavin nucleotides in yeast mitochondria, J. Biol. Chem. 271 (1996) 7392–7397.
[57] Y. Wan, R.A. Saleem, A.V. Ratushny, O. Roda, J.J. Smith, C.H. Lin, J.H. Chiang, J.D. Aitchison, Role of the histone variant H2A.Z/Htz1p in TBP recruitment, chromatin dynamics, and regulated expression of oleate-responsive genes, Mol. Cell. Biol. 29 (2009) 2346–2358.
[58] J. Wang, B. Zhang, S. Chen, Oleaginous yeast *Yarrowia lipolytica* mutants with a disrupted fatty acyl-CoA synthetase gene accumulate saturated fatty acid, Proc. Biochem. 46 (2011) 1436–1441.
[59] H. Yazawa, H. Kumagai, H. Uemura, Characterization of triglyceride lipase genes of fission yeast *Schizosaccharomyces pombe*, Appl. Microbiol. Biotechnol. 96 (2012) 981–991.
[60] Z. Zou, F. Tong, N.J. Faergeman, C. Børsting, P.N. Black, C.C. DiRusso, Vectorial acylation in *Saccharomyces cerevisiae*. Fat1p and fatty acyl-CoA synthetase are interacting components of a fatty acid import complex, J. Biol. Chem. 278 (2003) 16414–16422.
[61] J. Folch, M. Lees, G.H. Sloane Stanley, A simple method for the isolation and purification of total lipids from animal tissues, J. Biol. Chem. 226 (1957) 497–509.
[62] C.W. van Roermund, L. Ijlst, T. Wagemans, R.J. Wanders, H.R. Waterham, A role for the human peroxisomal half-transport ABCD3 in the oxidation of dicarboxylic acids, Biochim. Biophys. Acta. 2014 (1841) 563–568.
[63] J.Y. Choi, C.E. Martin, The Saccharomyces cerevisiae FAT1 gene encodes an acyl-CoA synthetase that is required for maintenance of very long chain fatty acid levels, J. Biol. Chem. 274 (1999) 4671–4683.